Bardo, Ameline, Dunmore, Christopher J., Cornette, Raphaël and Kivell, Tracy L. (2023) *Morphological integration and shape covariation between the trapezium and first metacarpal among extant hominids.* American Journal of Biological Anthropology, 183 (3). ISSN 2692-7691.

RESEARCH ARTICLE

AMERICAN JOURNAL OF
BIOLOGICAL ANTHROPOLOGY
The Official Journal of the American Association of Biological Anthropologists
WILEY

Morphological integration and shape covariation between the trapezium and first metacarpal among extant hominids

Ameline Bardo[1,2] | Christopher J. Dunmore[2] | Raphaël Cornette[3] |
Tracy L. Kivell[2,4]

[1]Département Homme et Environnement, UMR 7194 – HNHP, CNRS-MNHN, Musée de l'Homme, Paris, France

[2]Skeletal Biology Research Centre, School of Anthropology and Conservation, University of Kent, Canterbury, Kent, UK

[3]Institute of Systematic, Evolution, Biodiversity (ISYEB), UMR 7205–CNRS/ MNHN/UPMC/EPHE, National Museum of Natural History, Paris, France

[4]Department of Human Origins, Max Planck Institute for Evolutionary Anthropology, Leipzig, Germany

Correspondence
Ameline Bardo, Département Homme et Environnement, UMR 7194 – HNHP, CNRS-MNHN, Musée de l'Homme, 17 place du Trocadéro, 75016, Paris, France.
Email: abardo@mnhn.fr

Funding information
Fyssen Foundation Research Fellowship; H2020 European Research Council, Grant/Award Number: 819960

Abstract

Objectives: The shape of the trapezium and first metacarpal (Mc1) markedly influence thumb mobility, strength, and the manual abilities of extant hominids. Previous research has typically focused solely on trapezium-Mc1 joint shape. Here we investigate how morphological integration and shape covariation between the entire trapezium (articular and non-articular surfaces) and the entire Mc1 reflect known differences in thumb use in extant hominids.

Materials and Methods: We analyzed shape covariation in associated trapezia and Mc1s across a large, diverse sample of *Homo sapiens* (n = 40 individuals) and other extant hominids (*Pan troglodytes*, n = 16; *Pan paniscus*, n = 13; *Gorilla gorilla gorilla*, n = 27; *Gorilla beringei*, n = 6; *Pongo pygmaeus*, n = 14; *Pongo abelii*, n = 9) using a 3D geometric morphometric approach. We tested for interspecific significant differences in degree of morphological integration and patterns of shape covariation between the entire trapezium and Mc1, as well as within the trapezium-Mc1 joint specifically.

Results: Significant morphological integration was only found in the trapezium-Mc1 joint of *H. sapiens* and *G. g. gorilla*. Each genus showed a specific pattern of shape covariation between the entire trapezium and Mc1 that was consistent with different intercarpal and carpometacarpal joint postures.

Discussion: Our results are consistent with known differences in habitual thumb use, including a more abducted thumb during forceful precision grips in *H. sapiens* and a more adducted thumb in other hominids used for diverse grips. These results will help to infer thumb use in fossil hominins.

KEYWORDS
African apes, morphological integration, orangutans, thumb, trapeziometacarpal joint

1 | INTRODUCTION

Unlike other extant hominids (great apes), the increased reliance on bipedal locomotion over the past six million years of human evolution

2 | WILEY | AMERICAN JOURNAL OF BIOLOGICAL ANTHROPOLOGY
The Official Journal of the American Association of Biological Anthropologists

BARDO ET AL.

facilitated the evolution of enhanced dexterity in *Homo sapiens* (Bardo et al., 2017; Crast et al., 2009; Marzke, 1997; Napier, 1993). Modern human manipulative abilities are traditionally linked to specific morphological features of the hand, such as short fingers with broad finger tips, proximodistally-aligned radiocarpal joints, and a mobile and powerful thumb, all of which are considered beneficial for forceful precision grips, particularly between the palmar pads of the thumb and one or more fingers (Almécija et al., 2010; Almécija et al., 2015; Karakostis et al., 2021; Marzke, 1997, 2009; Marzke et al., 1992; Napier, 1956). This morphology and enhanced dexterity are linked to the evolution of increasingly complex tool technologies within the hominin clade, particularly stone tool-related behaviors (Kivell, 2015; Marzke, 1997; Napier, 1960; Susman, 1998; Tocheri et al., 2008). In contrast, although other hominids are dexterous relative to most other non-human primates (Fragaszy & Crast, 2016; Heldstab et al., 2016; Torigoe, 1985; but see Gumert et al., 2009; Tan et al., 2015; Truppa et al., 2019), they must also use their hands for a variety of locomotor behaviors. Thus, non-human great ape hand morphology may be described as a compromise between the functional requirements of terrestrial and arboreal locomotion and manipulation (Dunmore et al., 2019; Dunmore, Bardo, et al., 2020; Kivell, 2015; Marzke, 2013; Preuschoft & Chivers, 2012; Tuttle, 1969).

Within this context, several studies have investigated the functional morphology of hominoid hand bones with regards to both locomotion (Begun & Kivell, 2011; Bird et al., 2021; Dunmore et al., 2019; Tuttle, 1967; Vanhoof et al., 2021) and manipulative behaviors (Dunmore, Bardo, et al., 2020; Kivell, 2015; Lewis, 1989; Skinner et al., 2015; van Leeuwen et al., 2019) to make more informed reconstructions of hand use from the fossil record (Dunmore, Skinner, et al., 2020; Galletta et al., 2019; Marchi et al., 2017;

Niewoehner, 2001; Rose, 1992; Susman, 1998; Tocheri et al., 2003; Trinkaus, 1989). A strong focus of this research has been on thumb morphology as its opposition to the fingers plays a crucial role in human manipulation (Almécija et al., 2010; Hamrick et al., 1998; Marchi et al., 2017; Marzke et al., 2010; Napier, 1952; Susman, 1998; Tocheri et al., 2003; Tocheri et al., 2005; Trinkaus, 1989). The degree of mobility at the trapeziometacarpal (TMc) joint between the distal trapezium (i.e., trapezium's Mc1 facet) and proximal base of the first metacarpal (Mc1) (i.e., Mc1's trapezium facet) has received substantial attention (e.g., Lewis, 1977; Marzke et al., 2010; Napier, 1955; Rose, 1992) (Figure 1), but other morphological aspects of these two bones are comparatively understudied. Here, we use a 3D geometric morphometric (GM) approach to quantify the articular and non-articular morphology of the entire trapezium and the entire Mc1 – hereafter named, the trapeziometacarpal (TMc) complex – in extant hominids to investigate if they are morphologically integrated and how their shapes covary, with the aim of examining the potential link between thumb use and phenotypic trait covariance.

Napier (1961) was among the first to comparatively investigate the morphology of the TMc joint among primates, focusing on the reciprocal concavo-convex articular surfaces and the level of their congruence. Napier (1961) concluded that only catarrhines are capable (to varying degrees) of thumb opposition, a combined movement of abduction, flexion and ulnar rotation (see also Jouffroy & Lessertisseur, 1959). Rafferty (1990) showed that the TMc joint is generally saddle-shaped in all anthropoid primates and that the lack of congruence in the radioulnar aspect of the surfaces, which allows the ulnar rotation necessary for thumb-finger opposition, is present only in catarrhines. In extant hominids, the trapezium's Mc1 facet is dorsally extended to permit a greater range of extension of the Mc1 (Rafferty, 1990) and, from the joint
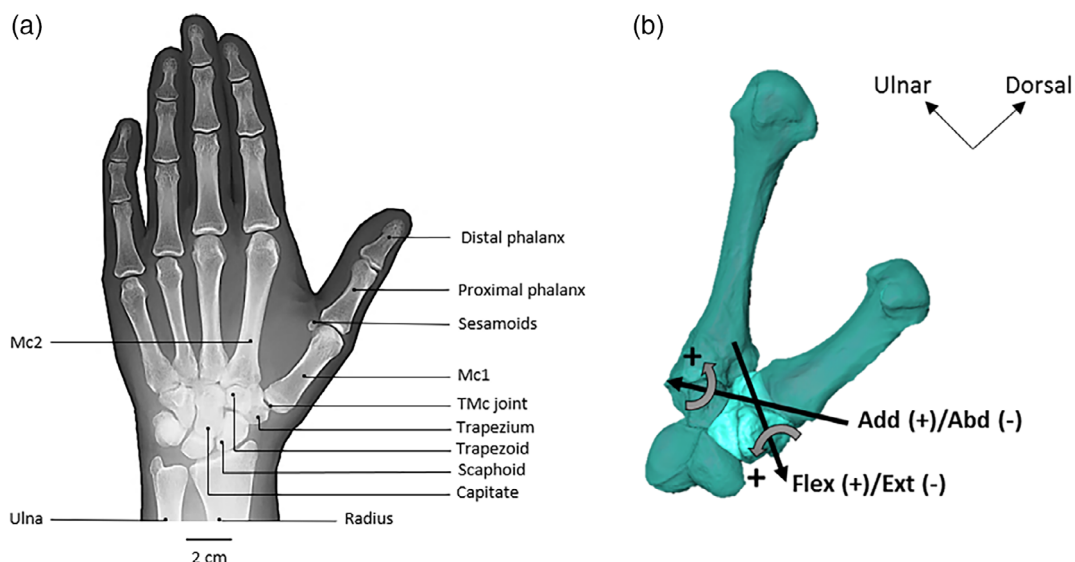
FIGURE 1 Human hand morphology and thumb motion. (a) Radiograph of a human left hand in dorsal view showing the location of the trapezial-Mc1 (TMc) joint and other hand bones of the radiocarpal region and thumb. (b) An illustration of TMc joint motion (following Halilaj et al., 2014) in humans. The bones are shown in neutral position and the directions of joint motion are labeled as adduction (Add+) and abduction (Abd−), as well as flexion (Flex+) and extension (Ext−) (Not depicted is the axial rotation caused by the incongruence between the two articular facets of the TMc joint). The strong complex of ligaments and tendons is not considered in this illustration.

morphology, Rose (1992) estimated greater abduction-adduction and rotation than in non-hominid primates. Moreover, Rose (1992) estimated a greater range of flexion/extension and abduction/adduction in humans than in the other great apes, while Tuttle's (1969) measurements from cadaveric specimens found a greater range of extension and adduction in *Pongo* than in the other non-human great apes. Perhaps due to this larger range of motion in hominids, including humans, the TMc joint is also surrounded by a strong complex of ligaments and tendons that stabilize the thumb as it opposes the fingers (Bettinger et al., 1999; Lewis, 1977, 1989; Nanno et al., 2006; Scheuer & Black, 2000; Schwarz & Taylor, 1955; van Leeuwen et al., 2018; van Leeuwen et al., 2019).

The concavo-convex curvature of the TMc joint as well as the complexity of radiocarpal articulations, in which the trapezium articulates with the scaphoid (or os centrale), trapezoid, and capitate, makes this anatomical region challenging to quantify using traditional linear measurements. Three-dimensional approaches have recently been applied to the TMc joint (Marzke et al., 2010; Tocheri, 2007), the radiocarpal articulations (Orr et al., 2010; Tocheri et al., 2003, 2005), the Mc1's trapezium surface alone (Marchi et al., 2017; Niewoehner, 2005), the non-articular Mc1 body alone (Bowland et al., 2021; Morley et al., 2022), the distal (phalangeal) Mc1 surface alone (Galletta et al., 2019), and the overall shape of the Mc1 including a focus of its entheses (Kunze et al., 2022). For example, using mathematical modeling, Marzke et al. (2010) quantified variation in the 3D curvature of both surfaces of the TMc saddle-shaped joint, showing that the human joint surfaces are flatter, both dorsopalmarly and radioulnarly, than in other extant hominids. This human morphology is thought to facilitate forceful precision and power gripping during human manipulative activities by distributing large axial loads to the trapezium over a large surface area, with a joint curved enough to limit mobility and provide stability (Marzke et al., 2010). Using 3D GM, Marchi et al. (2017) showed that, in comparison to other hominids, the modern human Mc1 facet for the trapezium is less curved and radially extended, suggesting a greater range of abduction. They also showed that *Gorilla* have greater radioulnar and dorsopalmar curvature associated with a more projecting palmar beak compared with *Pan* and *Pongo*, which they suggest may facilitate forceful food processing (Marchi et al., 2017), such as counter pressure by the thumb when pulling vegetation held within the mouth (Byrne et al., 2001; Neufuss et al., 2019).

A similar GM analysis of the Mc1s distal articulation with the pollical proximal phalanx found that, in comparison to other hominids, modern humans have a flatter articular facet, a larger epicondyle surface area and a larger radial palmar condyle, suggesting a lower range of motion at the thumb metacarpophalangeal (MCP) joint that would better resist loads associated with forceful precision grips (Galletta et al., 2019). They also found that *Pongo* have a relatively round and domed thumb MCP joint with smaller epicondyles and palmar condyles compared to African apes, suggesting higher motion at this joint (Galletta et al., 2019). This increased MCP joint mobility may help to balance some of the functional constraints of a short thumb (Almécija et al., 2015) and more limited TMc joint motion in *Pongo* (Rafferty, 1990).

Tocheri and colleagues (Tocheri et al., 2003, 2005) used 3D watershed-based hybrid segmentation method to quantify variation in the size and orientation of trapezium and trapezoid joints (radiocarpal joints) among hominids. They showed that the trapezoid has relatively

larger articular surfaces for the scaphoid and Mc2 in non-human hominids, whereas modern humans have larger joint surfaces for the scaphoid and the first metacarpal on their trapezium (Tocheri et al., 2003, 2005). In addition, the articular facets throughout the radiocarpal region, including those of the proximal Mc2 for the trapezium and for the capitate, are more proximodistally-oriented in modern humans than in the other hominids, suggesting biomechanical advantages for radioulnarly-directed load transmission in the human wrist during powerful thumb use (Lewis, 1989; Tocheri, 2007; Tocheri et al., 2005).

The above studies provide valuable information about morphological variation in the primate TMc complex but each has focused on a single bone or joint, while the movement and loading of the thumb is in part delimited by the interaction of the two bones of the TMc complex. To our knowledge, the 3D quantification of the combined overall shape of the trapezium and the Mc1 in hominids has not been investigated. As suggested by Marzke (2005), functional inferences from isolated bones or joints cannot accurately capture the full interaction between bones, especially those involved in complex manipulative behaviors. Here we use 3D surface GM and covariation analyses to test the degree of morphological integration and quantify the pattern of shape covariation exhibited between associated trapezia and Mc1s (i.e., the total TMc complex) in each extant hominid (*Pongo*, *Gorilla*, *Pan* and *H. sapiens*).

The concepts of morphological integration and modularity in biology are used to describe processes that underlie phenotypic trait changes that occur during the evolution (Olson & Miller, 1958). These morphological changes result from interactions of the biological processes generating the phenotypic structures under investigation, such as common functional, developmental, or genetic factors (Cheverud, 1996; Klingenberg, 2008). Accordingly, organisms are composed of sets of phenotypic traits that evolve with varying degrees of independence from each other (Cheverud, 1996). Morphological integration is the tendency for specific morphological features to significantly covary, which is the extent to which different traits are linked to one another (strength of covariation). The pattern of this integration describes the manner in which these traits change together (the patterns of covariation) (Klingenberg, 2008). For example, one might expect the TMc joint (like all joints in the skeleton) should be strongly integrated to function effectively (i.e., the two articular surfaces must be integrated to some degree for the joint to work) and, particularly, given its functional importance to thumb mobility and stability. As the TMc joint of the trapezium becomes wider the pattern of this integration means that the opposing TMc joint on the Mc1 might also become wider. In contrast, modularity refers to a lack of significant morphological integration and distinguishes a suite of highly-integrated features within a particular anatomical region (or "module") from other modules (Klingenberg, 2009, 2010). That is, "modularity is about differences in the degree of integration of parts within and between sets of traits" (Klingenberg, 2008: 116). For example, morphological integration may be stronger within the TMc joint compared with integration across the whole TMc complex, creating a 'TMc joint module' within the TMc complex due to functional, developmental, or genetic factors.

In this study, we quantify covariance between the overall shape of the trapezium and the Mc1, including its articular (i.e., the trapezium's

facets for the Mc1, scaphoid, capitate and trapezoid, and the Mc1's trapezium and proximal phalanx facets) and non-articular shape (including, for example, shape variation in the trapezium's tubercle and robusticity of Mc1 shaft). The quantification of covariance between the trapezium and Mc1 allows us to test how strongly the two bones are integrated and to examine the specific pattern of covariation (i.e., how the shape of one bone is reflected in the shape of the other). We hypothesize that strength and pattern of covariance between the trapezium and the Mc1 will reflect variation in observed thumb use and associated manipulative abilities across taxa. We assume that the shapes and orientations of the carpometacarpal and carpal articular facets reflect, at least in part, adaptations to the magnitude and trajectory of forces experienced by the thumb and wrist during hand use (in both manipulative and locomotor behaviors) (Lewis, 1977; Niewoehner, 2001; 2005; Tocheri et al., 2005). Studies of the anatomy and kinematics of the human TMc joint (e.g., Halilaj et al., 2014; Hollister et al., 1992; see as well a recent study in bonobos, van Leeuwen et al., 2019), demonstrate that the abduction-adduction axis principally moves the head of the rigid first metacarpal in a radio-ulnar direction, rolling the first metacarpal base so that different areas of the articular surface are closest to the trapezium. Similarly, the TMc joint flexion-extension axis runs through the trapezium in a dorso-palmar direction, moving and pitching the first metacarpal base palmarly or dorsally (Buford et al., 1990; Hollister et al., 1992). Within this context, we assume that specific patterns of articular facet shape covariation will reflect, at least in part, the limit of possible thumb postures of a particular TMc morphology. In turn, these extreme thumb postures imply force trajectories that are principally directed proximally along the rigid long axis of Mc1 diaphysis (Rolian et al., 2011), and subsequently through the proximal trapezial facets into the rest of the carpus. This assumption follows a fundamental concept of solid mechanics (i.e., normal stress in axial loading; Wallace, 2019). We assume that the force trajectories going through large articular facets are more effectively transmitted than through narrow facets, as for a given force as pressure would be decreased, and therefore we assume that, this specific TMc morphology would facilitate specific thumb postures. We acknowledge this is a gross simplification of TMc joint biomechanics, especially in the absence of soft tissue anatomy which is also critical to joint mobility and stability (Cooney et al., 1981; Marzke et al., 2010; Tocheri, 2007; van Leeuwen et al., 2019), but this approach does provide indications of joint loading from engineering principles, in the absence of hominid wrist biomechanical data not yet available (Kivell et al., 2022; van Leeuwen et al., 2019; van Leeuwen et al., 2021; but see, for the range of motion at the midcarpal joint, Orr, 2017; Orr et al., 2010). We also quantify the covariance between the surfaces of the TMc joint alone, to test the hypothesis that morphological integration and, hence, modularity is greater at this joint relative to the whole TMc complex given the functional importance of this articulation to thumb mobility and stability.

1.1 | Predictions

The first aim of this study is to test whether morphological integration is higher in the TMc complex or the TMc joint, across and within each great ape species. We predict:

1. Stronger morphological integration at the TMc joint relative to the total TMc complex across hominids given the 'singular function' of this joint and the importance of functional coherence between the complementary articular surfaces in all species (Lewis, 1977; Tocheri, 2007; Tocheri et al., 2005).
2. Stronger morphological integration in modern humans, in both the TMc joint and TMc complex, due their more forceful and complex thumb postures relative to other hominids (e.g., Bardo et al., 2016; Bardo et al., 2017; Crast et al., 2009; Elliott & Connolly, 1984).
3. Stronger morphological integration in African apes (*Pan* and *Gorilla*) versus orangutans (*Pongo*) given the enhanced manipulation of the former, documented both in the wild (e.g., Byrne et al., 2001; Marzke et al., 2015; Neufuss et al., 2019) and in zoo-based studies (e.g., Bardo et al., 2016, 2017; Crast et al., 2009).

The second aim is to characterize the covarying morphology in the TMc complex and the TMc joint of each species and how this relates to thumb postures and grips typical for each species. We assume that the shapes of the articular facets can reflect, at least in part, adaptations to the range of motion, and the orientation of the articular facets can reflect the trajectories of forces experienced by the thumb and wrist during specific hand use.

1. We predict that: each genus will present a specific shape covariation pattern for the overall shape of the TMc complex that will reflect observed differences in manipulative abilities and locomotor grasping (e.g., Bardo et al., 2017; Byrne et al., 2001; Christel, 1993; Feix et al., 2016; Gérard et al., 2022; Marzke & Wullstein, 1996; Neufuss et al., 2017; Neufuss et al., 2019; Pouydebat et al., 2009). That is, when the covarying shapes of each species TMc complex are manually articulated, we predict a hypothetical range of motion that facilitates thumb placement in the most frequent postures observed in living individuals of the species. Further, we predict that when the covarying TMc complex is articulated in the most frequently observed thumb posture for the taxon, the estimated trajectory of force (approximated by the Mc1 long axis) will pass through the center of articular facets that are arranged so that each is oriented orthogonal to the force vector. Specifically, we predict:
   a. modern humans will show shape covariation within the TMc complex facilitating greater *abduction* of the Mc1 than in the other hominids (Dunmore, Bardo, et al., 2020; Tuttle, 1969), which is a posture typically used during forceful precision grips (D'Agostino et al., 2017; Feix et al., 2016; Marzke, 1997, 2013; Napier, 1956). Further, we predict shape covariation in modern humans that results in radioulnarly-oriented joint facets for the Mc1, trapezoid, and scaphoid, which should result primarily in distal-to-proximal compressive loading when the thumb is in an abducted position (thereby minimizing potentially damaging shear forces on the joints at the base of the thumb).
   b. *Gorilla* and *Pan* will reflect shape covariation within the TMc complex facilitating adduction and flexion, following previous morphological studies (Dunmore, Bardo, et al., 2020; Rose, 1992;

Tuttle, 1969) and what we know about their thumb use (Bardo et al., 2017; Christel, 1993; Crast et al., 2009; Neufuss et al., 2017). Further, we predict shape covariation in *Gorilla* and *Pan* that results in obliquely-oriented (relative to the radio-ulnar plane) joint facets for the Mc1, trapezoid, and scaphoid, which should result primarily in distal-to-proximal compressive loading when the thumb is in an adducted position.

c. *Pongo* shape covariation will reflect extension and adduction, according to previous morphological studies (Rose, 1992; Tuttle, 1969) and their known habitual thumb use (Bardo et al., 2017; Christel, 1993; Pouydebat et al., 2009). Further, we predict shape covariation in *Pongo*, as for African great apes, that results in obliquely-oriented (relative to the radioulnar plane) joint facets for the intercarpal facets, which should result primarily in distal-to-proximal compressive loading when the thumb is in an adducted position.

2. Finally, regarding the TMc joint specifically, we predict that modern humans will demonstrate shape covariation at the TMc joint surfaces with more dorsopalmarly and radioulnarly extended and flatter articular facets, which when articulated, allows for a greater range of abduction/adduction and flexion/extension than the other great apes (Marchi et al., 2017; Marzke et al., 2010; Rafferty, 1990; Rose, 1992; van Leeuwen et al., 2019).

2 | MATERIALS AND METHODS

2.1 | Specimens

The study sample includes n = 125 individuals with an associated trapezium and Mc1 across the following taxa: *Homo sapiens* (n = 40 individuals), *Pan troglodytes* (n = 16) *Pan paniscus* (n = 13), *Gorilla gorilla gorilla* (n = 27), *Gorilla beringei* (n = 6), *Pongo pygmaeus* (n = 14) and *Pongo abelii* (n = 9) (detailed in Table S1). All the specimens are adult individuals with no obvious signs of pathology and species samples are sex balanced as much as possible. Only the *P. paniscus* sample was substantially sex-biased with more females (Table S1). All non-human hominids were wild-caught. The modern human individuals derive from diverse populations both geographically and temporally, including Europe, Central Africa and North America as well as Russia and the Chatham Islands and range from 5th century to 20th century time periods. All trapezia and Mc1s derive from the right side to control for any asymmetric morphology that may result from the documented prevalence (∼90%) of right-handedness across modern human populations (Annett, 1985; Perelle & Ehrman, 1994), while non-human hominids do not show a population-level hand-preference (Papademetriou et al., 2005).

H. sapiens samples are curated at the Musée de l'Homme in Paris (France), Georg-August-Universität in Göttingen (Germany), Naturhistorisches Museum Wien (Austria), University of Florence (Italy), the University of Kent in Canterbury (UK), and the University of Cambridge (UK). The non-human hominid samples are curated at the following institutions: Muséum National d'Histoire Naturelle (MNHN,

Paris, France), Powell Cotton Museum (Birchington, UK), Royal Museum for Central Africa (Tervuren, Belgium), the Smithsonian National Museum of Natural History (Washington, D.C., USA), Naturalis Biodiversity Center (Leiden, Netherlands), State Zoological Collection (München, Germany), and Naturmuseum Senckenberg (Frankfurt, Germany) (Table S1).

2.2 | Acquisition of the 3D models

The 3D digitized bones were obtained through three different methods (Table S1): photogrammetry, laser surface scanning, and micro-computed tomography (μCT) and computed tomography (CT) scanning. The 3D models from photogrammetry (pixel size 50 μm) were obtained with a Nikon D5100 DSLR camera with a resolution of 24 megapixels and a focal length fixed to 55 mm (Objectif AF-S DX 18–55 mm VR II). Fifty pictures were captured on both sides of the object from different viewpoints and the Agisoft PhotoScan software (©2014 Agisoft LLC) was used to reconstruct the 3D models. The laser surface scans were obtained with a NextEngine laser scanner® (pixel size 125 μm). Twelve scans were taken at different positions on both sides of the bone and then merged using the ScanStudio HD PRO software®. The specimens obtained via μCT were scanned with a BIR ACTIS 225/300, Diondo D3, or a Skyscan 1172 high-resolution micro-computed tomography scanner at the Department of Human Evolution, Max Planck Institute for Evolutionary Anthropology, Germany, or with the Nikon 225/XTH scanner at the Cambridge Biotomography Centre, University of Cambridge, UK. The specimens were scanned at 100–160 kV and 100–140 μA, using a brass or copper filter of 0.25–0.5 mm. The reconstructed scans were with an isometric voxel size range of 28–41 μm. The *Pongo* and the *Gorilla* specimens were CT scanned on a Siemens Somatom Emotion CT scanner (slice thickness 1 mm, slice increment 0.1 mm, voltage 110 kV, current 70 mA, reconstructing algorithm H50 moderately sharp kernel, pixel size 600 μm). Scanning artifacts or anomalies in the polygonal mesh from all the 3D models were corrected using Geomagic Wrap 2015 (3D Systems, Inc) software. Though the sample contains data from several acquisition methods, many studies have found that the measurement error introduced by this approach is minor (Pietrobelli et al., 2022; Robinson & Terhune, 2017; Tocheri et al., 2011; Waltenberger et al., 2021), and so all imaging data were pooled.

2.3 | Geometric morphometrics

Due to the shape complexity of the trapezium and Mc1, we quantified shape covariation using a GM approach (Zelditch et al., 2012) with both 3D anatomical landmarks and 3D sliding semi-landmarks on curves and surfaces (Gunz & Mitteroecker, 2013). 3D sliding semi-landmarks allow one to accurately describe anatomical zones of high biological interest (e.g., joint surfaces) that are devoid of anatomical landmarks (Cornette et al., 2013).

First, we created a template of landmarks for both bones (Figure 2 and Table 1), taking into consideration the variation in morphology in all hominids in our sample. Anatomical landmarks and sliding semi-landmarks on curves and surfaces were manually placed on the surface meshes, without texture, in IDAV Landmark software (Wiley et al., 2005) following Cornette et al. (2013). Nine type II anatomical landmarks (Bookstein, 1991) were defined on each bone (Table 1). Curves were defined at the margins of articular surfaces and were bordered by anatomical landmarks as recommended by Gunz et al. (2005). The curve length was 3–8 landmarks (Table 1). Surface sliding semi-landmarks were placed at a high spatial density with approximately equidistant spacing. The number of anatomical landmarks, sliding semi-landmarks on curves and on surfaces for each bone surface are listed in Table 1.

To assess intra-observer error, the set of anatomical and curve landmarks were placed six times on one individual of each genus (i.e., *Homo*, *Gorilla*, *Pan*, and *Pongo*) over several days (Fernández et al., 2015). General Procrustes Analysis (GPA) produced Procrustes co-ordinates for all of the repeat specimens, which were then subject to Principal Component Analyses (PCAs). The differences in shape between repeated landmark sets on single bones were significantly smaller than those between bones in each species (Figure S1) as assessed via a MANOVA on the first two principal components ($p < 0.001$).

Second, anatomical landmarks and sliding semi-landmarks on curves were digitized manually on all specimens following the templates described above. Next, surface sliding semi-landmarks were projected from a thin plate spline deformation of the template onto the bone surfaces (Gunz & Mitteroecker, 2013) using the "Morpho" package (Schlager, 2017). Then, configuration of the semi-landmarks on surfaces and curves were relaxed onto each surface of both bones (Mc1 and trapezium) by minimizing bending energy (Schlager, 2017). A sliding procedure was then performed using the "Morpho" package (Botton-Divet et al., 2015; Schlager, 2017) by minimizing the Procrustes distance (Gunz et al., 2005; Gunz & Mitteroecker, 2013). This sliding step allows the placement of geometrically homologous semi-landmarks on curves and surfaces (for details see Gunz et al., 2005; Gunz & Mitteroecker, 2013). After sliding, a GPA (Rohlf & Slice, 1990) was performed with all the specimens and for each bone with the "geomorph" package (Adams et al., 2020). Bone size was measured using centroid size (Bookstein, 1991). After this step, all landmarks and sliding semi-landmarks were then analyzed as traditional 3D landmarks. The same procedure was followed for the trapezial-Mc1 joint surfaces landmark data set.

2.4 | Statistical analysis

Two-Block Partial Least Squares (2B-PLS) analyses on Procrustes co-ordinates (Rohlf & Corti, 2000), implemented in "geomorph" (Adams et al., 2020), were used to investigate the degree of morphological integration and patterns of shape covariation between the trapezium and the Mc1 (i.e., the TMc complex), and between

the facets of the TMc joint. This method reduces the covariance between two data matrices—in this case Procrustes co-ordinates of the trapezium and Mc1 (Cornette et al., 2013; Polly, 2008)— to a few variables (PLS axes) that explain most of the covariance between both shapes. To quantify the degree of morphological integration between the trapezium and the Mc1, we performed the "integration.test" from the geomorph package (Adams et al., 2020) that used a 2B-PLS analysis. However, as the partial least-squares coefficient (rPLS) is dependent on both the number of specimens and number of variables (Adams & Collyer, 2016), the levels of integration between species showing a significant effect were also compared using the Z-score generated by the "compare.pls" function in geomorph (Adams et al., 2020). These tests were performed on both the overall data set representing shape covariation between the whole trapezium and the whole Mc1 (trapeziometacarpal complex), and on the data set representing just the trapezio-Mc1 joint surfaces (trapeziometacarpal joint).

We tested for significant inter-specific differences in the pattern of shape covariation by comparing mean species PLS scores via omnibus and pairwise one-way permutational MANOVAs (1000 permutations) on the Euclidean distance matrices of the first two PLS axes scores, independently (each accounting for more than 10% of the total variance). As the assumption of multivariate homogeneity of variance was violated for the first axis of the PLS of the TMc joint ($p < 0.01$) we used non-parametric (permutational) tests for all analyses, and Bonferroni correction was applied to all pairwise results, to ensure valid comparisons. These permutational MANOVAs were run using the "Vegan" (Oksanen et al., 2018) and "RVAideMemoire" (Hervé & Hervé, 2020) packages.

To visualize the shape deformations associated with the extremes of the PLS axes, the "Morpho" package was used (Schlager, 2017). The coordinates computed for each extreme of the axes were then used to compute a Thin Plate Spline deformation of the bone template (Schlager, 2017). All analyses were performed in the R environment (R Core Team, 2019).

Both deformed shapes (i.e., the entire Mc1 and trapezium) are generated separately and not in articulation. Moreover, the TMc complex is surrounded by a complex of ligaments that constrain and stabilize movement at the TMc joint but which are not assessed in this study. Therefore, accurately illustrating the range of motion at the TMc joint based on shape deformation obtained via the 2B-PLS analyses is not possible. Instead, we illustrate anatomically coherent close-packed manual articulations of the quantitatively covarying TMc joint, in adduction/abduction thumb postures following a previous study in humans (Halilaj et al., 2014). This articulation then permits visualization of the possible trajectories of forces through the shape deformations associated with the extremes of the PLS axes, as we assume that force (without considering the soft tissues) is assumed to be principally directed proximally along the long axis of Mc1 diaphysis. We visualize only the abduction/adduction postures and potential associated force trajectories as these are modeled to variously pass through the covarying proximal articular surfaces of the TMc complex, whereas the flexion/extension force
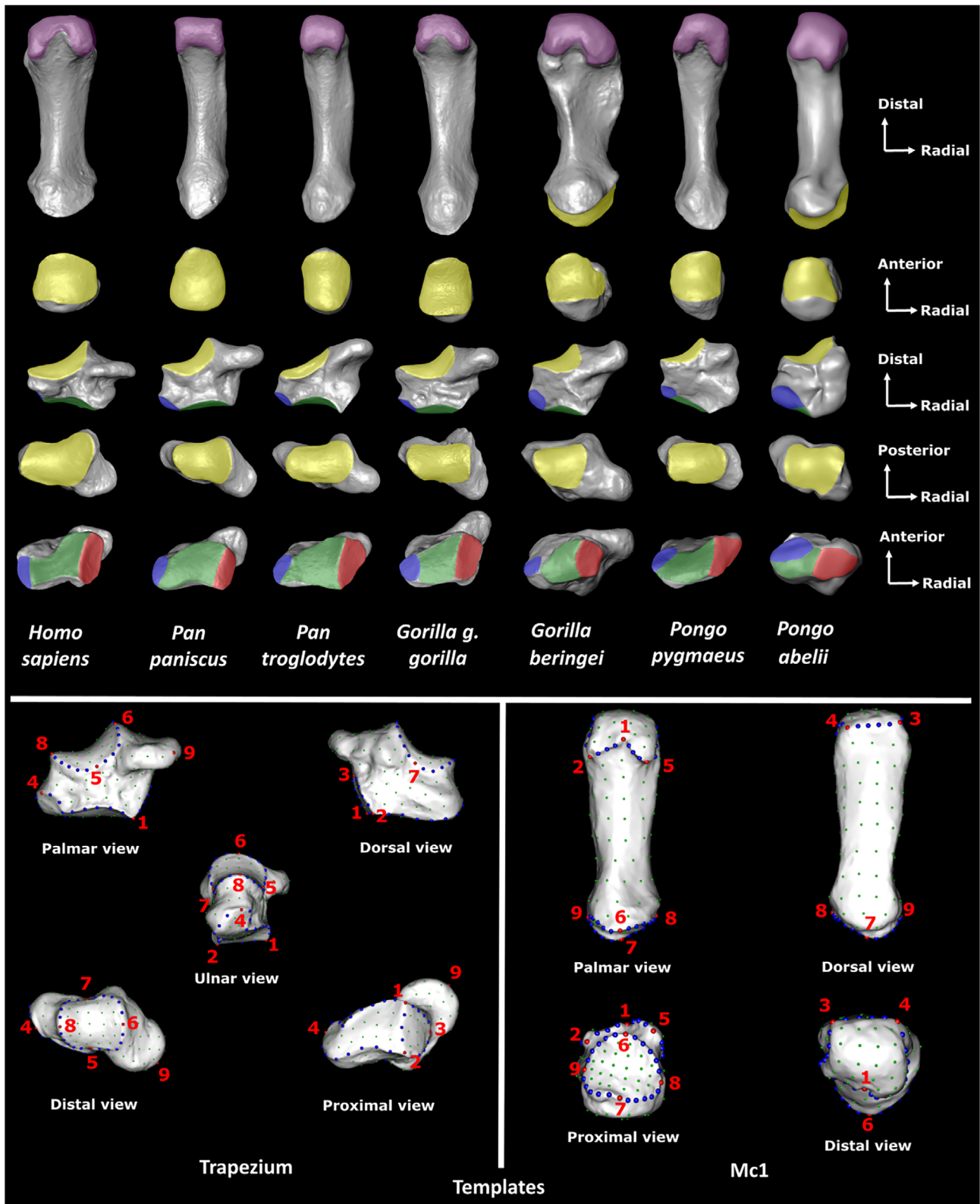
BARDO ET AL.

AMERICAN JOURNAL OF
BIOLOGICAL ANTHROPOLOGY
The Official Journal of the American Association of Biological Anthropologists

WILEY 7

FIGURE 2 Comparative morphology and landmarks of the hominid right trapezium and right first metacarpal (Mc1). Inter-specific shape comparison of the Mc1 in palmar view (1st row) and proximal view (2nd row) and of trapezium in palmar view (3rd row), proximal row (4th row) and distal view (5th row) in a representative individual in each species. Color Key: purple, distal metacarpophalangeal joint; yellow, trapezial-Mc1 joint; blue, Mc2 facet; green, trapezoid facet; red, scaphoid facet. At bottom of figure, landmark templates for each bone used in our analyses to quantify shape covariation. Anatomical landmarks are in red, sliding semi-landmarks on curves are in blue and sliding semi-landmarks on surfaces are in green (defined in Table 1). Images not to scale.

8 | WILEY— AMERICAN JOURNAL OF BIOLOGICAL ANTHROPOLOGY
The Official Journal of the American Association of Biological Anthropologists

BARDO ET AL.

TABLE 1 Definition of the anatomical landmarks (Lm) and sliding semi-Lm on curves of the trapezium and the Mc1 following Marchi et al. (2017), Galletta et al. (2019) and Dunmore, Bardo, et al. (2020). Curves are bordered by anatomical Lm with the first number corresponding of the initial anatomical Lm and the second of the terminal anatomical Lm, or initiated and terminated with the same anatomical Lm. The trapezium contains 145 sliding semi-Lm on surfaces and the Mc1 138. The distal joint of the trapezium and the proximal joint of the Mc1 contains the exact same number of Lm: 4 anatomical Lm, 20 sliding semi-Lm on curves, and 24 sliding semi-Lm sliding on surfaces.

	Landmark	Definition
Trapezium *Total 200 points*	1	The most anterior aspect of the scaphoid articular surface
	2	Most posterior aspect of the scaphoid articular surface
	3	Most distal aspect of the scaphoid articular surface
	4	Most distal aspect of the Mc2 articular surface
	5	Most palmar aspect of the distal articular surface
	6	Most radial aspect of the distal articular surface
	7	Most dorsal aspect of the distal articular surface
	8	Most ulnar aspect of the distal articular surface
	9	Point of maximum of curvature of the tip of the tubercle of the trapezium
Curves *46 semi-Lm*	1–2, 2–3, 3–1	3 curves around the scaphoid articular surface
	1–4, 4–2	2 curves around the trapezoid and the Mc2 articular surfaces
	5–6, 6–7, 7–8, 8–5	4 curves around the Mc1 articular surface (distal joint of the trapezium)
Mc1 *Total 187 points*	1	The point of maximum curvature on the interepicondylar ridge between Points 2 and 5
	2	Most proximal point under the ulnar palmar epicondyle (anterior eminence)
	3	Most ulnarly projecting point on the dorsal aspect of the distal articular surface
	4	Most radially projecting point on the dorsal aspect of the distal articular surface
	5	Most proximal point under the radial palmar epicondyle (anterior eminence)
	6	Most palmar aspect of the proximal articular surface, the 'tip' of the palmar beak
	7	Most dorsal aspect of the articular surface on the metacarpal base
	8	Most radial aspect of the articular surface on the metacarpal base (proximal joint)
	9	Most ulnar aspect of the articular surface on the metacarpal base
Curves *40 semi-Lm*	1–2, 2–3, 3–4, 4–5, 5–1	5 curves around the metacarpal head (distal joint)
	6–8, 8–7, 7–9, 9–6 s	4 curves around the trapezial joint surface (proximal joint)

trajectories are transferred only through the trapezium-trapezoid joint.

2.5 | Allometry

We assessed allometry because it may be an important influence on morphological integration in the TMc complex and TMc joint alone, and the pattern of shape covariation between the Mc1 and the trapezium in each species. To visually assess the range of variation in size across our sample, box-and-whisker plots of the $\log_{10}$ centroid size for each species and bone were created. To assess the degree of morphological change in response to size change, we performed 2B-PLS of Procrustes co-ordinates of each bone on centroid size. If the strength of the covariation between shape and size, in either bone, was less than the covariation between bone shapes, as measured by the 2B-PLS above (Adams & Collyer, 2016), we assumed allometry was not strong enough to have a substantial effect on the results. These analyses were performed with the geomorph package (Adams et al., 2020), following the same process than to quantify the degree of morphological integration, and run for both the TMc complex and the TMc joint separately.

3 | RESULTS

3.1 | Degree of morphological integration

3.1.1 | Trapeziometacarpal complex

The 2B-PLS analysis revealed significant morphological integration between the entire trapezium and Mc1 across all species studied (rPLS = 0.846, $Z = 11.6$, $p = 0.001$). No significant morphological integration between the overall shapes of the trapezium and the Mc1 was found within each species ($p > 0.05$; Table 2).

3.1.2 | Trapeziometacarpal joint

The 2B-PLS analysis revealed significant morphological integration between the trapezium's Mc1 facet and the Mc1's trapezium facet across all species studied (rPLS = 0.82, $Z = 10.1051$, $p = 0.001$). We found that the trapezium's Mc1 facet and the Mc1's trapezium facet were significantly morphologically integrated for *H. sapiens* ($p < 0.01$) and *G. g. gorilla* ($p < 0.05$; Table 2), but no significant morphological

BARDO ET AL.

AMERICAN JOURNAL OF
BIOLOGICAL ANTHROPOLOGY
The Official Journal of the American Association of Biological Anthropologists

WILEY 9

TABLE 2 Results of the morphological integration tests between the whole TMc complex and for the TMc joint, for each species.

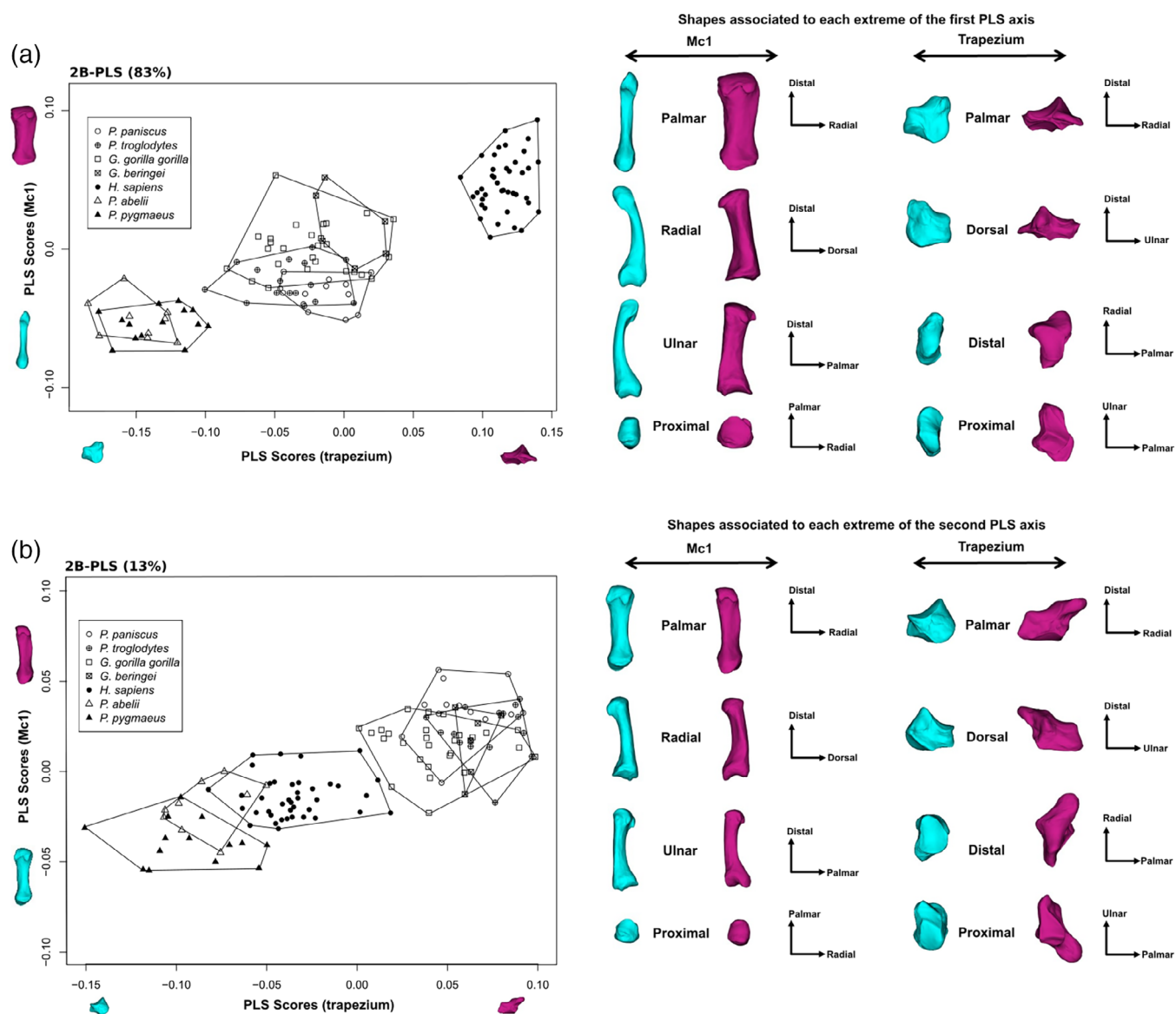|	Whole TMc complex			TMc joint		
	r-PLS	Z scores	P value	r-PLS	Z scores	P value
H. sapiens	0.677	0.879	0.200	0.712	2.713	**0.007**
P. paniscus	0.872	0.769	0.210	0.810	1.338	0.090
P. troglodytes	0.863	0.814	0.220	0.784	0.590	0.280
G. g. gorilla	0.758	0.814	0.200	0.757	1.722	**0.048**
G. beringei	0.960	0.537	0.080	0.936	1.228	0.130
P. abelii	0.927	0.660	0.280	0.884	0.428	0.350
P. pygmaeus	0.801	0.160	0.440	0.836	1.571	0.060

FIGURE 3 2B-PLS of shape covariation between the TMc complex across species. (a) 1st PLS axis and (b) 2nd PLS axis. The figures on the right represent the bone shapes associated with each negative (in blue) and positive (in purple) extreme of the shape covariation axes, in different anatomical views (right hand bones). All shapes are scaled to approximately the same length.

integration was found in the other taxa ($p > 0.05$). We found no evidence of significant differences in levels of integration between *H. sapiens* and *G. g. gorilla* ($p > 0.05$).

3.2 | Shape covariation

3.2.1 | Trapeziometacarpal complex

The two first PLS axes cumulatively explained 96% of the total covariance between the whole trapezium and the Mc1. The first PLS axis (PLS1) explained 83% of the total covariance and separated *Pongo* (negative side of this axis) from *H. sapiens* (positive side of this axis), while African apes were intermediate on the PLS axis and overlapped with each other (Figure 3). All species showed significantly different patterns of shape covariation except between *P. troglodytes* and *G. g. gorilla*. There were no significant differences between species of the same genus (Table 3). The first PLS axis reflected both shape differences as well as the relative orientation of the joints. *Pongo* (negative side of this axis) were distinguished by a gracile and proximodistally-curved Mc1 shaft, a strongly domed Mc1 head which was ulnarly-oriented relative to its base, and a Mc1's trapezium facet that is strongly dorsopalmarly concave and radioulnarly convex with an

extension of the radial border (Figure 3a). The covarying trapezium in *Pongo* (negative side of this axis) was distinguished by being robust and radioulnarly short, forming roughly a square, with a small tubercle, and intercarpal joints that are obliquely-oriented relative to the radio-ulnar plane, and a trapezio-Mc2 joint that is parasagittally oriented and palmarly extended (Figure 3a). In contrast, *H. sapiens* (positive side of this axis) was distinguished by a robust and proximodistally straight Mc1 shaft, a relatively flat metacarpophalangeal facet, and a shallow curvature to the dorsopalmarly concave and radioulnarly convex Mc1's trapezium facet, which is radially extended with a pronounced palmar beak (Figure 3a). The covarying trapezium in *H. sapiens* (positive side of this axis) was distinguished by being radioulnarly elongated and proximodistally narrow, with a pronounced tubercle, a dorsoradially elongated Mc1 facet, intercarpal joints oriented closer to the radioulnar plane, and a more proximodistally-oriented trapezial-Mc2 joint (Figure 3a).

The second PLS axis (PLS2) explained 13% of the total covariance and separated *Pongo* (negative side of the axis) from the African apes (positive side of this axis) (Figure 3b). *H. sapiens* overlapped with *P. abelii* but all non-human hominids were significantly different from *H. sapiens* ($p < 0.01$; Table 3). African apes were significantly different from *Pongo* ($p < 0.05$). All African apes overlapped but *G. g. gorilla* and *P. troglodytes* showed significant differences in their patterns of shape

TABLE 3 Significant results of subsequent omnibus and pairwise one-way permutational MANOVAs on the first two PLS axes testing differences of shape covariation between the two bones of the whole TMc complex and TMc joint across species. Table shaded rows are for within genera analyses. All values marked in bold where significant at $p < 0.05$, and are reported subsequent to a Bonferroni correction for the comparisons across species.

	Whole TMc complex		TMc joint	
	PLS1	**PLS2**	**PLS1**	**PLS2**
H. sapiens/P. paniscus	**0.002**	**0.002**	**0.002**	**0.002**
H. sapiens /P. troglodytes	**0.002**	**0.002**	**0.002**	0.139
H. sapiens /G. g. gorilla	**0.002**	**0.002**	**0.002**	**0.002**
H. sapiens /G. beringei	**0.002**	**0.002**	**0.002**	1.000
H. sapiens /P. abelii	**0.002**	**0.002**	**0.002**	1.000
H. sapiens /P. pygmaeus	**0.002**	**0.002**	**0.002**	**0.002**
P. paniscus/P. troglodytes	0.280	0.391	1.000	**0.002**
P. paniscus/ G. g. gorilla	**0.010**	0.078	**0.002**	**0.010**
P. paniscus/ G. beringei	**0.004**	1.000	0.372	**0.002**
P. paniscus/ P. abelii	**0.002**	**0.002**	1.000	**0.002**
P. paniscus/ P. pygmaeus	**0.002**	**0.002**	**0.002**	**0.002**
P. troglodytes/ G. g. gorilla	0.088	**0.008**	**0.008**	**0.002**
P. troglodytes/ G. beringei	**0.002**	1.000	1.000	1.000
P. troglodytes/ P. abelii	**0.002**	**0.002**	1.000	1.000
P. troglodytes/ P. pygmaeus	**0.002**	**0.002**	0.099	**0.002**
G. g. gorilla/ G. beringei	0.834	1.000	**0.002**	0.065
G. g. gorilla/ P. abelii	**0.002**	**0.002**	**0.019**	1.000
G.g. gorilla/ P. pygmaeus	**0.002**	**0.002**	**0.002**	1.000
G. beringei/ P. abelii	**0.008**	**0.017**	1.000	1.000
G. beringei/ P. pygmaeus	**0.002**	**0.002**	0.979	**0.002**
P. abelii/ P. pygmaeus	1.000	1.000	0.630	0.510

BARDO ET AL.

AMERICAN JOURNAL OF
BIOLOGICAL ANTHROPOLOGY
The Official Journal of the American Association of Biological Anthropologists

WILEY 11

covariation ($p < 0.05$). *Pongo* (negative side of this axis) was distinguished by a more radially-oriented Mc1 head relative to its base and an elongated ulnar palmar epicondyle, the trapezium facet was more strongly curved in the dorsopalmar direction than in the radioulnar direction and was more obliquely oriented relative to the radioulnar plane (Figure 3b). The covarying trapezium in *Pongo* (negative side of this axis) was robust and radioulnarly short with a small tubercle, had radioulnarly broad Mc1 and scaphoid facets that were more obliquely-oriented relative to the radioulnar plane, and a Mc2 facet which was oriented parasagittally and palmarly extended (Figure 3b). In contrast, *Pan* and *Gorilla* (positive side of this axis) were distinguished by a robust Mc1 shaft relative to *Pongo*, which appears to be driven primarily by a more well-developed crest for the insertion of the *m. opponens pollicis* and a pronounced palmar beak that is slightly ulnarly oriented relative to its head (Figure 3b). The covarying trapezium in *Pan* and *Gorilla* (negative side of this axis) was distinguished by being radioulnarly elongated and dorsopalmarly narrow, resulting in dorsopalmarly narrow intercarpal joints that were more obliquely-oriented relative to the radioulnar plane, a Mc2 facet that was

oriented closer to the radioulnar plane, and a more pronounced tubercle (Figure 3b).

Figure 4 depicts hypothetical trajectories of forces from abduction/adduction thumb postures based on the shape deformations (Mc1 and the covarying trapezium) associated with the extremes of PLS1 and PLS2. For the shape deformations associated with the negative side of PLS1 (*Pongo*), the potential force vector for the Mc1 adduction would pass through the trapezium to its trapezio-scaphoid joint, while in Mc1 abduction, the potential force vectors would pass through the trapezium to its trapezio-Mc2 joint. For the shape deformations associated with the positive side of PLS1 (*H. sapiens*), the potential force vectors for the Mc1 adduction would pass through the trapezium to its trapezio-scaphoid joint, and for the Mc1 abduction would pass through the trapezium to its trapezio-trapezoid joint. For the shape deformations associated with the negative side of PLS2 (*Pongo*), the potential force vectors for the Mc1 adduction would pass through the trapezium to its trapezio-scaphoid joint, and for the Mc1 abduction would pass through the trapezium to its trapezio-trapezoid joint. For the shape deformations associated with the positive side of
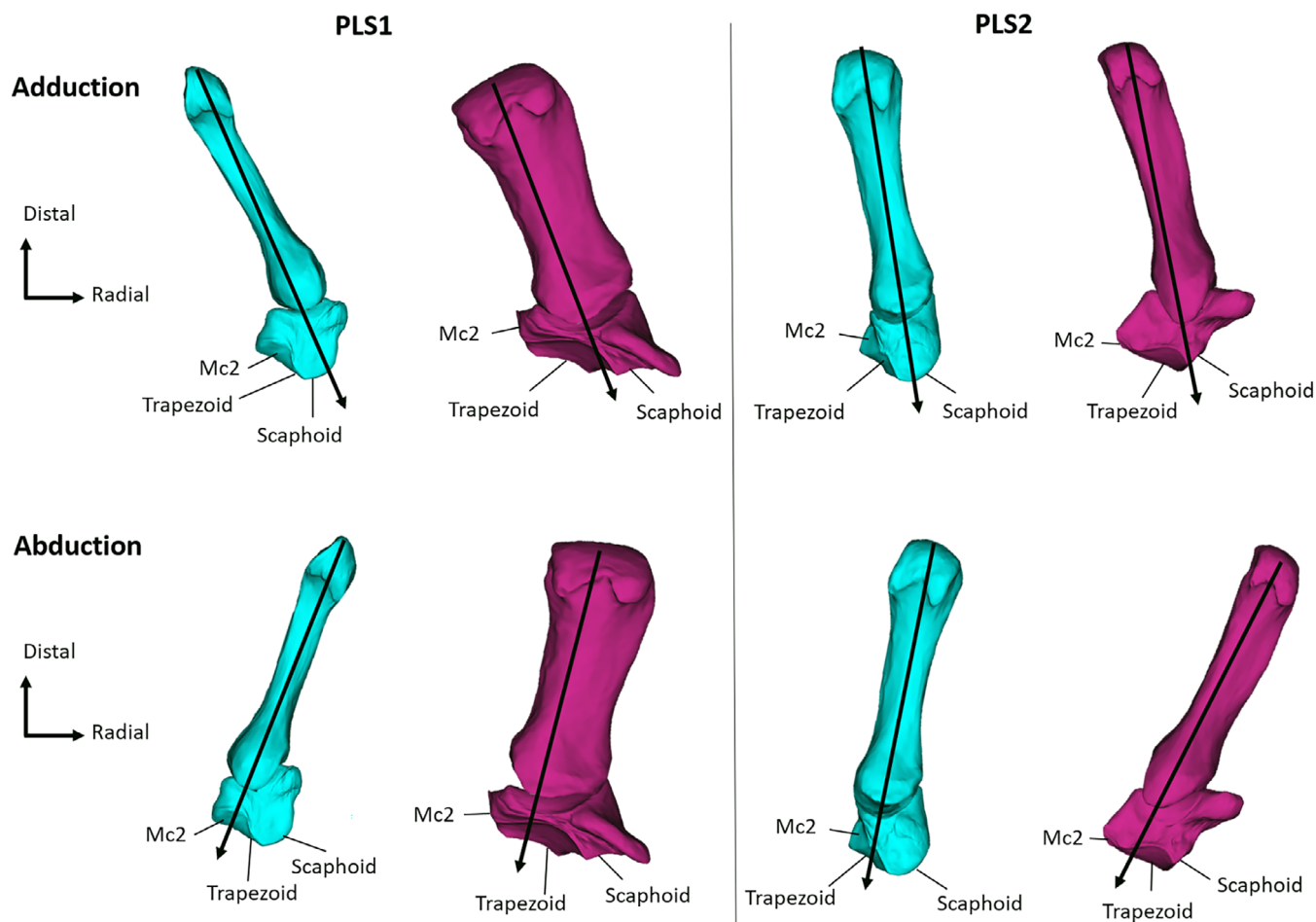

FIGURE 4 Illustration of possible adduction/abduction postures of the TMc complex (following Halilaj et al., 2014) according to the shape covariation associated with each positive (purple) and negative (blue) extremes of the first and second PLS axes. The associated hypothetical trajectories of force vector are assumed to be principally directed proximally along the long axis of Mc1 diaphysis. For each shape configuration a direction of force transmission from the Mc1 to the trapezium is suggested (black arrow). The illustration is not scaled.

PLS2 (*Pan & Gorilla*), the potential force vectors for the Mc1 adduction would pass through the trapezium to its trapezio-scaphoid joint, and for the Mc1 abduction would pass through the trapezium to its trapezio-trapezoid joint.

3.2.2 | Trapeziometacarpal joint

The first two PLS axes explained 88% of the total covariance between the Mc1's trapezium facet and the trapezium's Mc1 facet. The first PLS axis (PLS1) explained 74% of the total covariance and separated *H. sapiens* (negative side of this axis) from *G. g. gorilla* (positive side of this axis), while the other hominids fell out as intermediate and substantially overlapped (Figure 5a). All non-human hominids showed significant differences with *H. sapiens* (*p* < 0.01; Table 3). *P. paniscus*

showed significant differences with *G. g. gorilla* and *P. pygmaeus*, while *P. troglodytes* showed significant differences only with *G. g. gorilla* (*p* < 0.01). Within genera analyses revealed that only *G. g. gorilla* and *G. beringei* were significantly different (*p* < 0.01). In *H. sapiens* (negative side of this axis) the trapezial-Mc1 joint was distinguished by being radially extended and having flatter dorsopalmar curvature (Figure 5a). In contrast, *G. g. gorilla* (positive side of this axis) showed a trapezial-Mc1 joint that is more curved dorsopalmarly and radioulnarly as well as dorsally and ulnary extended, and with a pronounced palmar beak on the Mc1 (Figure 5a).

The second PLS axis (PLS2) explained 14% of the total covariance and separated some *Pongo* and *G. g. gorilla* (negative side of this axis) from *P. paniscus* (positive side of this axis), while *H. sapiens*, *G. beringei* and most *P. troglodytes* specimens fell out as intermediate along this PLS axis (Figure 5b). *P. paniscus* was significantly different from all
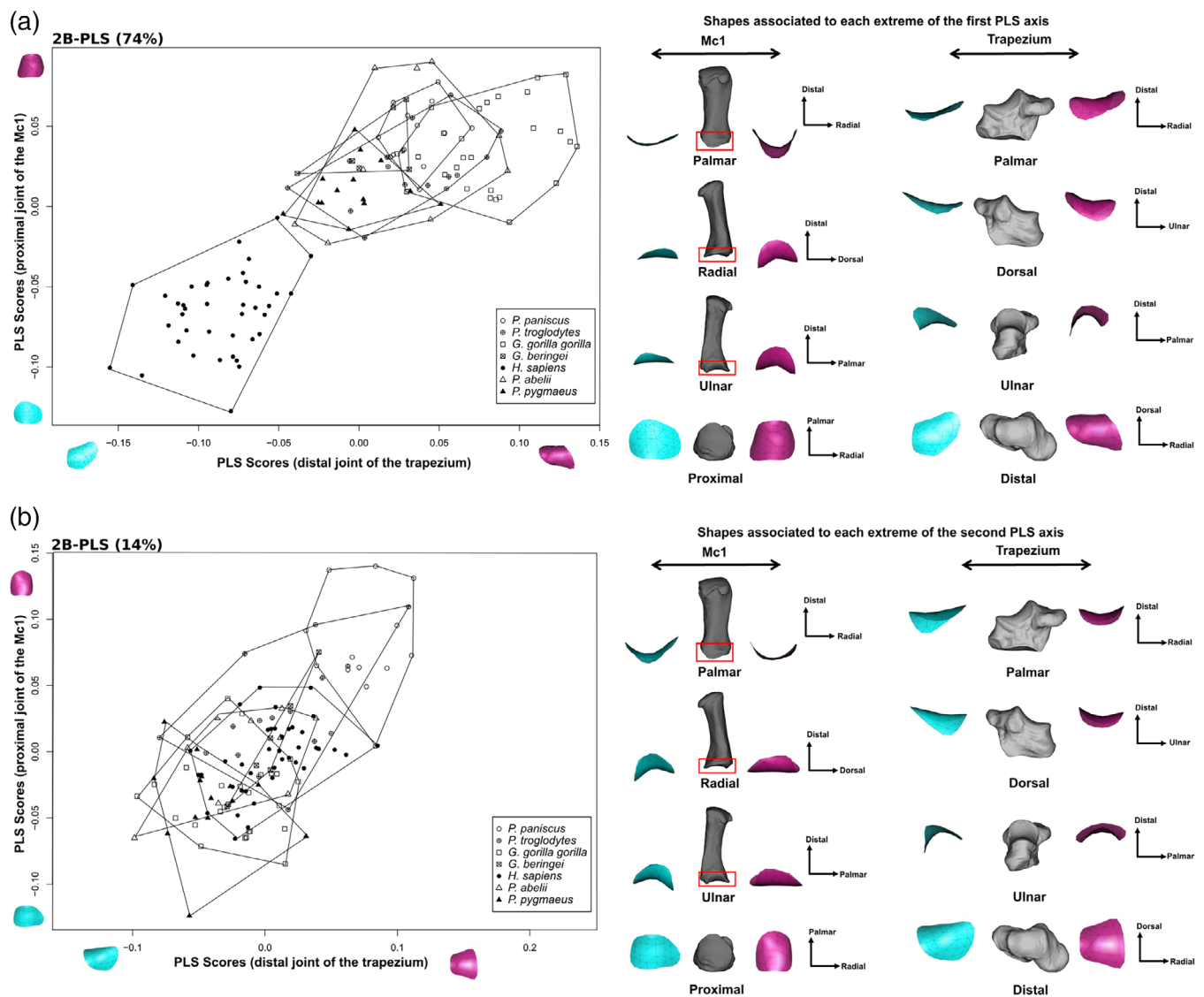

FIGURE 5 2B-PLS of shape covariation between the TMc joint across species. (a) 1st PLS axis and (b) 2nd PLS axis. The figures on the right represent the bone shapes associated with each negative (in blue) and positive (in purple) extreme of the shape covariation axes in different anatomical views (right hand bones). The full bones in gray are depicted with each surface to aid interpretation. All shapes are scaled to approximately the same length.

other species ($p < 0.05$; Table 3), *H. sapiens* and *P. troglodytes* were significantly different from *G. g. gorilla* and *P. pygmaeus* ($p < 0.01$), and *G. beringei* was significantly different from *P. pygmaeus* ($p < 0.01$). *Pongo* and *G. g. gorilla* (negative side of this axis) were distinguished by a radioulnarly broader and dorsopalmarly and radioulnarly curved TMc joint, a dorsally elongated Mc1 joint of the trapezium, and with a more pronounced palmar beak on the Mc1 than *P. paniscus* (Figure 5b). In contrast, *P. paniscus* (positive side of this axis) showed a TMc joint that is dorsopalmarly elongated and more strongly curved radioulnarly than dorsopalmarly (Figure 5b).

3.3 | Allometry

3.3.1 | Trapeziometacarpal complex

Different ranges of variation of the centroid size of the trapezium were found across the study taxa with *Gorilla* showing a higher mean centroid size than the other species, followed by *H. sapiens*, and then *Pongo* and *Pan* (Figure S2). Both *Pan* species showed smaller centroid size for the Mc1 than the other species (Figure S2).

The 2B-PLS analyses revealed significant covariation between centroid size and shape (GPA landmark coordinates) of the trapezium (rPLS = 0.471, $Z = 4.1852$, $p = 0.001$) and the Mc1 (rPLS = 0.399, $Z = 3.3608$, $p = 0.001$) (Figure S3), indicating an allometric effect for both bones. All taxa generally follow the regression line, for both the trapezium and Mc1, except *Pongo* for the trapezium (Figure S3). We found that shape covariation between the overall trapezium and Mc1 (Figure 3) was significantly stronger than the covariation between the shape and the centroid size for the Mc1 ($Z = 5.03$, $p < 0.0001$) and for the trapezium ($Z = 6.50$, $p < 0.0001$).

3.3.2 | Trapeziometacarpal joint

The Mc1's trapezium facet and the trapezium's Mc1 facet showed a similar range of variation in centroid size between them for each species, with *Gorilla* and *H. sapiens* showing higher centroid sizes than *Pongo* and *Pan* (Figure S4).

The 2B-PLS analyses revealed significant covariation between centroid size and shape of the trapezium's Mc1 facet (rPLS = 0.472, $Z = 4.7947$, $p = 0.001$) and the Mc1's trapezium facet (rPLS = 0.588, $Z = 7.5232$, $p = 0.001$), indicating an allometric effect at this joint in all the species (Figure S5). We found that shape covariation between the two facets (Figure 5) was significantly stronger than the covariation between the shape and the centroid size for the trapezium's Mc1 facet ($Z = 2.70$, $p < 0.01$) and the Mc1's trapezium facet ($Z = 4.48$, $p < 0.0001$).

4 | DISCUSSION

We investigated variation in morphological integration and patterns of shape covariation between the entire trapezium and the entire

Mc1 (TMc complex) as well as the TMc joint alone across extant hominids, to better understand how this morphology reflects known differences in habitual thumb postures and, by extension, grips used by each taxon. We predicted that the TMc joint alone would show more integration than the TMc complex as a whole for each genus. This prediction was only partially supported as significant morphological integration was only found in the TMc joint of *H. sapiens* and *G. g. gorilla*. We predicted that *H. sapiens* would show stronger morphological integration relative to African apes, and that the latter would be more morphologically integrated than *Pongo*. We also predicted that each genus would present a specific pattern of shape covariation plausibly related to frequently observed thumb postures typical for each species. Our results supported our prediction of interspecific difference in shape covariation, but did not entirely support our expectation that *H. sapiens* will be more morphologically integrated. These results are discussed in more detail below.

4.1 | Morphological integration

We predicted stronger integration in the TMc complex for *H. sapiens* compared to the other hominids but found no significant morphological integration between the overall trapezium and Mc1 within any species. Either soft-tissues better explain the large force dissipation in *H. sapiens* than joint shape or the TMc joint is modular (i.e., morphological integration is concentrated within the TMc joint rather than across the whole TMc complex), or both. Our results partially supported our prediction that the TMc joint alone will show more integration than the TMc complex as a whole for each genus. Interestingly, we found that only *H. sapiens* and *G. g. gorilla* showed a significant morphological integration at the TMc joint. This result may be explained by different factors. First, this result could be due to the fact that, relative to other hominids, *G. g. gorilla* and *H. sapiens*, especially, have a relatively shorter metacarpus (Almécija et al., 2015) that facilitates thumb opposition to the fingers in a more favoring powerful precision grips (Feix et al., 2016) as well as a more robust Mc1 and trapezium (Lewis, 1989), and reflects (*H. sapiens*) and suggests (*G. g. gorilla*) greater loading of their thumb and TMc joint (Bardo et al., 2018). Zoo-housed *G. g. gorilla* are capable of using complex manipulation (Bardo et al., 2017). However, if this were the case, we would expect *G. beringei* to show the same results, especially as they are also capable of complex manipulation (Byrne et al., 2001; Neufuss et al., 2019) and have a relatively shorter palm (i.e., more human-like) than *G. g. gorilla* (Almécija et al., 2015), yet we did not find significant morphological integration for *G. beringei*. This result may be influenced by differences in sample size: *H. sapiens* and *G. g. gorilla* were the bigger samples in this study, while we had only six *G. beringei*, meaning less statistical power to find the same integration we found in *G. g. gorilla* (n = 27) (Grabowski & Porto, 2017). Smaller sample sizes may also explain why we did not find significant morphological integration in either species of *Pan* or *Pongo*. Second, significant morphological integration for *H. sapiens* and *G. g. gorilla* could be influenced by methodology since a constant number of landmarks will necessarily sample

14 | WILEY— **AMERICAN JOURNAL OF BIOLOGICAL ANTHROPOLOGY**
The Official Journal of the American Association of Biological Anthropologists

BARDO ET AL.

less in a larger surface or redundantly oversample a smaller surface (Dunmore, Bardo, et al., 2020; Tocheri et al., 2005). Third, the significant integration of the *H. sapiens* and *G. g. gorilla* TMc joint, and the non-significant morphological integration for the whole bones, could be related. The trapezium and the Mc1 may contain at least two distinct modules, each with different functions: (1) the total TMc complex, including muscle attachment areas (i.e., entheses), that help to dissipate and transmit force, and (2) the TMc joint itself, that dictates (together with the associated soft tissues) the range of motion and probably also the position of most frequent loading. This hypothesis requires further investigation by quantifying modularity within the TMc complex across hominids and potentially integrating the study of muscle attachment areas (e.g., Karakostis et al., 2017) with the 3D GM analyses (Kunze et al., 2022).

4.2 | Shape covariation and functional interpretations

4.2.1 | Trapeziometacarpal complex

The results support our prediction that the overall shape of the TMc complex will show significant differences in shape covariation across taxa that are consistent with known differences in thumb use. The different patterns of shape covariation among hominids may result from a variety of factors: phylogeny, genetics, development, and/or functional requirements (Cheverud, 1996; Klingenberg, 2009, 2010). We found a combination of morphological patterns (shape and relative facet orientations) of the *H. sapiens* TMc complex that was clearly distinguished from that of other hominids, especially from *Pongo*, supporting previous research (Marchi et al., 2017; Marzke et al., 2010; Tocheri et al., 2005). The pattern of shape covariation of the *H. sapiens* TMc complex included a radially extended TMc joint and the radioulnar orientation of the trapezium's Mc1 and trapezoid facets. This *H. sapiens* morphology facilitates, more than great apes, an abducted thumb posture that would compressively load the TMc joint in manner which would then likely mainly load the trapezoidal facet. This facilitation is due the specific shape of the TMc joint as well as the size of the trapezoidal facet, which would likely create minimal shear forces, and provide a larger area for force disputation, reducing pressure for a given force, in this thumb posture. This TMc morphology likely effectively dissipates radioulnarly-directed load transmission in the human wrist during powerful thumb use as predicted and previously suggested (Bardo et al., 2020; Lewis, 1989; Tocheri et al., 2008; Figure 4). This result is consistent with the frequent use of forceful precision grips in *H. sapiens* with the thumb flexed and abducted in opposition to the other fingers (D'Agostino et al., 2017; Feix et al., 2016; Marzke, 1997, 2013; Napier, 1956) and with previous external and internal morphological analyses (Dunmore, Bardo, et al., 2020; Marchi et al., 2017; Rose, 1992; Stephens et al., 2018; Tocheri et al., 2003, 2005; Tuttle, 1969). In comparison, *Pongo* showed shape covariation in the TMc complex that would be advantageous for more adducted, rather than abducted, thumb

postures, with a load transmission that would pass through to their relatively large trapezial-scaphoid articular facet. Indeed, even though the Mc1's trapezium facet was radially elongated in *Pongo*, and therefore allowing greater abduction, their trapezial-Mc2 facet is oriented parasagittally and extended onto the palmar portion of the trapezium. This specific orientation would pass the potential force vector through the Mc2 and not the wrist, constraining the use of abducted thumb postures in *Pongo* and especially for precision grips. *Pongo* had the largest range of radioulnar movement, especially ulnarly (i.e., adduction), of all the non-human great apes in one study (Tuttle, 1969). This functional interpretation is consistent with their frequent use of the pad-to-side precision grips during manipulation (Bardo et al., 2017; Christel, 1993), although currently there are no studies of *Pongo* grip use during food processing or tool use in the wild. Their TMc joint morphology and their short thumbs (Almécija et al., 2015) would limit the types of precision grips that are possible, but the torsion of their Mc1 head (i.e., rotated ulnarly relative to the Mc1 base) may compensate the shape of their TMc complex and their short thumb by helping to slightly opposed the thumb to the index finger (Drapeau, 2015).

Our prediction that the pattern of shape covariation found in *Gorilla* and *Pan* will be different from the pattern of shape covariation in *Pongo* was partially supported. The second axis of the PLS explained a small part of the total covariance (13%) and separated *Pongo* from the African apes. Adduction seemed more advantageous with the shape covariation associated with *Pongo*, especially their broad trapezio-scaphoid facet could allow more optimally load transmission from the Mc1 to the trapezium and the other bones of the wrist compared to narrow trapezio-scaphoid facet in *Pan* and *Gorilla*. These results are consistent with behavioral studies showing more thumb opposition movements during food/tool manipulation in *Pan* and *Gorilla* than in *Pongo* (Bardo et al., 2017; Byrne et al., 2001; Christel, 1993; Marzke et al., 2015; Neufuss et al., 2019; Pouydebat et al., 2009; Pouydebat et al., 2011). It is interesting that *P. troglodytes*, which engage in more tool use in the wild (e.g., Boesch & Boesch, 1993; Goodall, 1964; Inoue-Nakamura & Matsuzawa, 1997; McGrew, 2010; Sanz & Morgan, 2013), is not separated from other African apes. However, all non-human hominids have been shown to use tools in zoo environments with diverse grips involving different thumb postures (Bardo et al., 2016, 2017), though never with an abducted thumb, which seems to be specific *H. sapiens* posture (Bardo et al., 2017).

4.2.2 | Trapeziometacarpal joint

We expected that *H. sapiens* would show shape covariation at the TMc joint consistent with a greater range of thumb postures (adduction/abduction and flexion/extension) than the other great apes (Marchi et al., 2017; Marzke et al., 2010). Our predictions were partially supported. We found for the first axis of the PLS there was a clear separation between *H. sapiens* and the other hominids, in accord with Rose (1992) who found higher range of motion for

BARDO ET AL.

AMERICAN JOURNAL OF
BIOLOGICAL ANTHROPOLOGY —WILEY 15
The Official Journal of the American Association of Biological Anthropologists

humans than great apes. We found significant differences between *H. sapiens* and *G. g. gorilla* but few differences between non-human hominids. The shape covariation analysis showed that the TMc joint of *H. sapiens* and *G. g. gorilla* covary in significantly different ways, consistent with their disparate thumb postures and use (Bardo et al., 2017; Byrne et al., 2001; Feix et al., 2016; Marzke, 1997, 2013; Neufuss et al., 2019). The specific shape of the TMc joint of *H. sapiens* (radially extended) would be more advantageous for an abducted thumb posture than *G. g. gorilla*. This result is consistent with forceful opposition of the thumb against the pads of the fingers in *H. sapiens* (D'Agostino et al., 2017; Dunmore, Bardo, et al., 2020; Feix et al., 2016; Marchi et al., 2017). However, the pattern of shape covariation found in humans did not appear more advantageous for flexion and extension compared to the other great apes. In contrast, *G. g. gorilla* showed a TMc joint that was more dorsally and ulnary extended than *H. sapiens* and would be more advantageous for an adducted and extended thumb posture. *Gorilla* has been observed using a variety of hand grips during food proceeding (Byrne et al., 2001; Christel, 1993; Neufuss et al., 2019), tool use (Bardo et al., 2017), as well as during locomotion (Neufuss et al., 2017), which is consistent with their hand proportions and thumb morphology allowing a theoretically larger kinematic workspace and forceful grips compared to the other non-human hominids (Almécija et al., 2015; Bardo et al., 2018; Dunmore, Bardo, et al., 2020; Feix et al., 2015; Galletta et al., 2019). However, their pronounced palmar beak at the Mc1's trapezium facet, and their trabecular bone distribution, may support a "screw-home" mechanism of the TMc joint during ulnar rotation (pronation) of the Mc1 as is found in *H. sapiens* (D'Agostino et al., 2017), generating less flexed position than the other hominids (Dunmore, Bardo, et al., 2020). In summation, this clear separation in the pattern of shape covariation between *H. sapiens* and *G. g. gorilla*, is consistent with variation in their observed thumb postures and use (Bardo et al., 2017; Feix et al., 2016). Although our small sample of *G. beringei* did not show a similar significant pattern of shape covariation, it is important to note that all the studies of wild *Gorilla* hand use are on *G. beringei* (Byrne et al., 2001; Neufuss et al., 2017, 2019) and we currently have no information about *G. g. gorilla* dexterity in their natural environment. Therefore, we do not know if and how hand use between these taxa may differ.

Interestingly, even if the second PLS axis of the shape covariation at the TMc joint explained a small part of the total covariance (14%), we found a clear separation between *P. paniscus* and both *Pongo* and *G. g. gorilla*. While *Pongo* and *G.g. gorilla* show a pattern of shape covariation that would be more advantageous for extension (dorsally elongated Mc1 facet of the trapezium), *P. paniscus* has a TMc joint with a flatter dorsopalmar curvature which would be advantageous for larger loads distributed to the trapezium, providing more joint stability such as in humans (Marzke et al., 2010; Momose et al., 1999). Bonobos and humans were shown to have a similar overall TMc kinematics, but with humans exhibiting a higher range of motion in thumb extension than bonobos (van Leeuwen et al., 2019).

4.3 | Allometric effects on trapeziometacarpal complex covariation

We found a significant allometric effect in the shape of the trapezium and Mc1 but this effect was weaker than shape covariation between the two bones, indicating that variation in size alone cannot explain the differences shape covariation patterns found between species. Interestingly, *Pongo* was unique in our sample in showing no relationship between centroid size and shape for the trapezium (Figure S3), indicating a distinct lack of influence of size on shape in *Pongo* compared with other hominids. This may reflect the specific cuboidal shape of the trapezium in *Pongo* compared to a more radioulnarly-elongated trapezium for other hominids. Future analyses on potential allometric effects on hominid trapezia, as well as other carpals, is needed to determine if this is a common pattern across the *Pongo* carpus or if it reflects a specific allometric influence related to thumb size or use. Furthermore, although our sample sizes were not large enough to statistically test for differences between sexes in each genus, sex-related size differences may have an important influence on shape covariation, especially in taxa with strong sexual dimorphism (i.e., *Gorilla* and *Pongo*), that are worth exploring in future analyses.

5 | CONCLUSION

We found no significant morphological integration between the overall shapes of the trapezium and the Mc1 in hominids, but did find significant integration at the TMc joint in *H. sapiens* and *G. g. gorilla*. The shape covariation analysis revealed that these *H. sapiens* and *G. g. gorilla* thumbs covary in significantly different ways, which is consistent with variation in their observed thumb postures and use. Moreover, the lack of morphological integration in other species in TMc complex and TMc joint may suggest that the TMc joint is not just functionally integrated but is also a module in *H. sapiens* and *G. g. gorilla*. However, it is not yet understood why *G. beringei* does not show a similar pattern of morphological integration as its generic counterpart. The shape covariation analysis for the overall TMc complex showed different species-specific patterns that clearly distinguished *H. sapiens* from other extant hominids. Our results are consistent with a more abducted thumb used during forceful precision grips in *H. sapiens* and with a more adducted thumb in non-human hominids used for diverse grips. Moreover, the morphology of the TMc complex of *Pongo* appears to favor more thumb adduction than that of African apes, consistent with what we currently know about thumb use in each species. Although our understanding of hand and thumb use and biomechanics is well described for *H. sapiens* (Braido & Zhang, 2004; Bullock & Dollar, 2011; Elliott & Connolly, 1984; Exner, 1992), our knowledge in non-human hominids remains limited (e.g., Bardo et al., 2016, 2017; Byrne et al., 2001; Crast et al., 2009; Marzke et al., 2015). Future studies of hand and thumb use in extant hominids, particularly in natural environments, may provide more accurate information about the morpho-functional requirements of

16 | WILEY—**AMERICAN JOURNAL OF BIOLOGICAL ANTHROPOLOGY**
The Official Journal of the American Association of Biological Anthropologists

BARDO ET AL.

some manual abilities and improve our inferences of hand function from fossil remains (Kivell, 2015).

DATA AVAILABILITY STATEMENT

The data that support the findings of this study are available from the corresponding author upon reasonable request.

ORCID

Ameline Bardo https://orcid.org/0000-0003-1840-6423
Christopher J. Dunmore https://orcid.org/0000-0002-8634-9777
Raphaël Cornette https://orcid.org/0000-0003-4182-4201
Tracy L. Kivell https://orcid.org/0000-0001-5087-0897

REFERENCES

Adams, D. C., & Collyer, M. L. (2016). On the comparison of the strength of morphological integration across morphometric datasets. *Evolution*, *70*(11), 2623–2631.

Adams, D. C., Collyer, M. L., & Kaliontzopoulou, A. (2020). Geomorph: Software for geometric morphometric analyses. R package version 3.2.1. https://cran.r-project.org/package=geomorph

Almécija, S., Moya-Sola, S., & Alba, D. M. (2010). Early origin for human-like precision grasping: A comparative study of pollical distal phalanges in fossil hominins. *PLoS One*, *5*(7), e11727.

Almécija, S., Smaers, J. B., & Jungers, W. L. (2015). The evolution of human and ape hand proportions. *Nature Communications*, *6*(1), 1–11.

Annett, M. (1985). *Left, right, hand and brain: The right shift theory*. Psychology Press London.

Bardo, A., Borel, A., Meunier, H., Guéry, J. P., & Pouydebat, E. (2016). Behavioral and functional strategies during tool use tasks in bonobos. *American Journal of Physical Anthropology*, *161*(1), 125–140.

Bardo, A., Cornette, R., Borel, A., & Pouydebat, E. (2017). Manual function and performance in humans, gorillas, and orangutans during the same tool use task. *American Journal of Physical Anthropology*, *164*(4), 821–836.

Bardo, A., Moncel, M. H., Dunmore, C. J., Kivell, T. L., Pouydebat, E., & Cornette, R. (2020). The implications of thumb movements for Neanderthal and modern human manipulation. *Scientific Reports*, *10*(1), 1–12.

Bardo, A., Vigouroux, L., Kivell, T., & Pouydebat, E. (2018). The impact of hand proportions on tool grip abilities in humans, great apes and fossil hominins: A biomechanical analysis using musculoskeletal simulation. *Journal of Human Evolution*, *125*, 106–121.

Begun, D. R., & Kivell, T. L. (2011). Knuckle-walking in Sivapithecus? The combined effects of homology and homoplasy with possible implications for pongine dispersals. *Journal of Human Evolution*, *60*(2), 158–170.

Bettinger, P. C., Linscheid, R. L., Berger, R. A., Cooney, W. P., III, & An, K. N. (1999). An anatomic study of the stabilizing ligaments of the trapezium and trapeziometacarpal joint. *The Journal of Hand Surgery*, *24*(4), 786–798.

Bird, E. E., Kivell, T. L., & Skinner, M. M. (2021). Cortical and trabecular bone structure of the hominoid capitate. *Journal of Anatomy*, *239*(2), 351–373.

Boesch, C., & Boesch, H. (1993). Different hand postures for pounding nuts with natural hammers by wild chimpanzees. In H. Preuschoft & D. Chivers (Eds.), *Hands of primates* (pp. 31–43). Springer- Verlag.

Bookstein, F. L. (1991). *Morphometric tools for landmark data: Geometry and biology*. Cambridge University Press.

Botton-Divet, L., Houssaye, A., Herrel, A., Fabre, A. C., & Cornette, R. (2015). Tools for quantitative form description; an evaluation of different software packages for semi-landmark analysis. *PeerJ*, *3*, e1417.

Bowland, L. A., Scott, J. E., Kivell, T. L., Patel, B. A., Tocheri, M. W., & Orr, C. M. (2021). Homo Naledi pollical metacarpal shaft morphology is distinctive and intermediate between that of australopiths and other members of the genus *Homo*. *Journal of Human Evolution*, *158*, 103048.

Braido, P., & Zhang, X. (2004). Quantitative analysis of finger motion coordination in hand manipulative and gestic acts. *Human Movement Science*, *22*(6), 661–678.

Buford, W., Hollister, A., & Myers, L. (1990). Three dimensional computer simulation of thumb carpometacarpal kinematics. *Journal of Clinical Engineering*, *15*, 445–451.

Bullock, I. M., & Dollar, A. M. (2011). Classifying human manipulation behavior. In *2011 IEEE international conference on rehabilitation robotics* (pp. 1–6). IEEE.

Byrne, R. W., Corp, N., & Byrne, J. M. (2001). Manual dexterity in the gorilla: Bimanual and digit role differentiation in a natural task. *Animal Cognition*, *4*(3–4), 347–361.

Cheverud, J. M. (1996). Developmental integration and the evolution of pleiotropy. *American Zoologist*, *36*(1), 44–50.

Christel, M. (1993). Grasping techniques and hand preferences in Hominoidea. In H. Preuschoft & D. Chivers (Eds.), *Hands of primates* (pp. 91–108). Springer.

Cooney, W. P., Lucca, M. J., Chao, E. Y., & Linscheid, R. L. (1981). The kinesiology of the thumb trapeziometacarpal joint. *The Journal of Bone and Joint Surgery*, *63*(9), 1371–1381.

Cornette, R., Baylac, M., Souter, T., & Herrel, A. (2013). Does shape co-variation between the skull and the mandible have functional consequences? A 3D approach for a 3D problem. *Journal of Anatomy*, *223*(4), 329–336.

Crast, J., Fragaszy, D., Hayashi, M., & Matsuzawa, T. (2009). Dynamic in-hand movements in adult and young juvenile chimpanzees (*Pan troglodytes*). *American Journal of Physical Anthropology*, *138*(3), 274–285.

D'Agostino, P., Dourthe, B., Kerkhof, F., Stockmans, F., & Vereecke, E. E. (2017). In vivo kinematics of the thumb during flexion and adduction motion: Evidence for a screw-home mechanism. *Journal of Orthopaedic Research*, *35*(7), 1556–1564.

Drapeau, M. S. (2015). Metacarpal torsion in apes, humans, and early Australopithecus: Implications for manipulatory abilities. *PeerJ*, *3*, e1311.

Dunmore, C. J., Bardo, A., Skinner, M. M., & Kivell, T. L. (2020). Trabecular variation in the first metacarpal and manipulation in hominids. *American Journal of Physical Anthropology*, *171*(2), 219–241.

Dunmore, C. J., Kivell, T. L., Bardo, A., & Skinner, M. (2019). Metacarpal trabecular bone varies with distinct hand-positions used in hominid locomotion. *Journal of Anatomy*, *235*, 45–66.

Dunmore, C. J., Skinner, M. M., Bardo, A., Berger, L. R., Hublin, J.-J., Pahr, D. H., Rosas, A., Stephens, N. B., & Kivell, T. L. (2020). The position of *Australopithecus sediba* in fossil hominin hand-use diversity. *Nature Ecology & Evolution*, *4*, 911–918.

Elliott, J. M., & Connolly, K. J. (1984). A classification of manipulative hand movements. *Developmental Medicine and Child Neurology*, *26*, 283–296.

Exner, C. E. (1992). In-hand manipulation skills. In J. Case-Smith & C. Pehoski (Eds.), *Development of hand skills in the child* (pp. 1–11). American Occupational Therapy Association.

Feix, T., Kivell, T. L., Pouydebat, E., & Dollar, A. M. (2015). Estimating thumb–index finger precision grip and manipulation potential in extant and fossil primates. *Journal of the Royal Society Interface*, *12*(106), e20150176.

Feix, T., Romero, J., Schmiedmayer, H. B., Dollar, A. M., & Kragic, D. (2016). The grasp taxonomy of human grasp types. *IEEE Transactions on Human-Machine Systems*, *46*(1), 66–77.

Fernández, P. J., Almécija, S., Patel, B. A., Orr, C. M., Tocheri, M. W., & Jungers, W. L. (2015). Functional aspects of metatarsal head shape in humans, apes, and Old World monkeys. *Journal of Human Evolution*, *86*, 136–146.

Fragaszy, D. M., & Crast, J. (2016). Functions of the hand in primates. In T. K. Kivell, P. Lemelin, B. G. Richmond, & D. Schmitt (Eds.), *The evolution of the primate hand* (pp. 313–344). Springer.

Galletta, L., Stephens, N. B., Bardo, A., Kivell, T. L., & Marchi, D. (2019). Three-dimensional geometric morphometric analysis of the first metacarpal distal articular surface in humans, great apes and fossil hominins. *Journal of Human Evolution*, *132*, 119–136.

Gérard, C., Bardo, A., Guéry, J. P., Pouydebat, E., Simmen, B., & Narat, V. (2022). Manipulative repertoire of bonobos (*Pan paniscus*) in spontaneous feeding situation. *American Journal of Primatology*, *84*(7), e23383.

Goodall, J. (1964). Tool-using and aimed throwing in a community of free-living chimpanzees. *Nature*, *201*(4926), 1264–1266.

Grabowski, M., & Porto, A. (2017). How many more? Sample size determination in studies of morphological integration and evolvability. *Methods in Ecology and Evolution*, *8*(5), 592–603.

Gumert, M. D., Kluck, M., & Malaivijitnond, S. (2009). The physical characteristics and usage patterns of stone axe and pounding hammers used by long-tailed macaques in the Andaman Sea region of Thailand. *American Journal of Primatology*, *71*(7), 594–608.

Gunz, P., & Mitteroecker, P. (2013). Semilandmarks: A method for quantifying curves and surfaces. *Hystrix, the Italian Journal of Mammalogy*, *24*(1), 103–109.

Gunz, P., Mitteroecker, P., & Bookstein, F. L. (2005). Semilandmarks in three dimensions. In D. E. Slice (Ed.), *Modern morphometrics in physical anthropology* (pp. 73–98). Springer.

Halilaj, E., Rainbow, M. J., Got, C., Schwartz, J. B., Moore, D. C., Weiss, A. P. C., Ladd, A. L., & Crisco, J. J. (2014). In vivo kinematics of the thumb carpometacarpal joint during three isometric functional tasks. *Clinical Orthopaedics and Related Research*, *472*(4), 1114–1122.

Hamrick, M. W., Churchill, S. E., Schmitt, D., & Hylander, W. L. (1998). EMG of the human flexor pollicis longus muscle: Implications for the evolution of hominid tool use. *Journal of Human Evolution*, *34*(2), 123–136.

Heldstab, S. A., Kosonen, Z. K., Koski, S. E., Burkart, J. M., van Schaik, C. P., & Isler, K. (2016). Manipulation complexity in primates coevolved with brain size and terrestriality. *Scientific Reports*, *6*(1), 1–9.

Hervé, M., & Hervé, M. M. (2020). Package 'RVAideMemoire'. See https://CRANR-projectorg/package=RVAideMemoire

Hollister, A., Buford, W. L., Myers, L. M., Giurintano, D. J., & Novick, A. (1992). The axes of rotation of the thumb carpometacarpal joint. *Journal of Orthopaedic Research*, *10*(3), 454–460.

Inoue-Nakamura, N., & Matsuzawa, T. (1997). Development of stone tool use by wild chimpanzees (*Pan troglodytes*). *Journal of Comparative Psychology*, *111*(2), 159–173.

Jouffroy, F. K., & Lessertisseur, J. (1959). La main des lémuriens malgaches comparée à celle des autres primates. *Mémoires de l'Institut Scientifique de Madagascar, Série A*, *13*, 195–219.

Karakostis, F. A., Haeufle, D., Anastopoulou, I., Moraitis, K., Hotz, G., Tourloukis, V., & Harvati, K. (2021). Biomechanics of the human thumb and the evolution of dexterity. *Current Biology*, *31*(6), 1317–1325.

Karakostis, F. A., Hotz, G., Scherf, H., Wahl, J., & Harvati, K. (2017). Occupational manual activity is reflected on the patterns among hand entheses. *American Journal of Physical Anthropology*, *164*, 30–40.

Kivell, T. L. (2015). Evidence in hand: Recent discoveries and the early evolution of human manual manipulation. *Philosophical Transactions of the Royal Society of London B: Biological Sciences*, *370*(1682), 20150105.

Kivell, T. L., Baraki, N., Lockwood, V., Williams-Hatala, E. M., & Wood, B. A. (2022). Form, function and evolution of the human hand. *Yearbook Biological Anthropology*, 1–52.

Klingenberg, C. P. (2008). Morphological integration and developmental modularity. *Annual Review of Ecology, Evolution, and Systematics*, *39*, 115–132.

Klingenberg, C. P. (2009). Morphometric integration and modularity in configurations of landmarks: Tools for evaluating a priori hypotheses. *Evolution & Development*, *11*(4), 405–421.

Klingenberg, C. P. (2010). Evolution and development of shape: Integrating quantitative approaches. *Nature Reviews Genetics*, *11*(9), 623–635.

Kunze, J., Karakostis, F. A., Merker, S., Peresani, M., Hotz, G., Tourloukis, V., & Harvati, K. (2022). Entheseal patterns suggest habitual tool use in early hominins. *PaleoAnthropology*, *2022*(2), 195–210.

Lewis, O. J. (1977). Joint remodeling and the evolution of the human hand. *Journal of Anatomy*, *123*(1), 157–201.

Lewis, O. J. (1989). *Functional morphology of the evolving hand and foot*. Clarendon Press.

18 | WILEY AMERICAN JOURNAL OF BIOLOGICAL ANTHROPOLOGY The Official Journal of the American Association of Biological Anthropologists

BARDO ET AL.

Marchi, D., Proctor, D. J., Huston, E., Nicholas, C. L., & Fischer, F. (2017). Morphological correlates of the first metacarpal proximal articular surface with manipulative capabilities in apes, humans and South African early hominins. *Comptes Rendus Palevol*, 16(5–6), 645–654.

Marzke, M., Tocheri, M., Steinberg, B., Femiani, J., Reece, S., Linscheid, R., Orr, C. M., & Marzke, R. F. (2010). Comparative 3D quantitative analyses of trapeziometacarpal joint surface curvatures among living catarrhines and fossil hominins. *American Journal of Physical Anthropology*, 141(1), 38–51.

Marzke, M. W. (1997). Precision grips, hand morphology, and tools. *American Journal of Physical Anthropology*, 102(1), 91–110.

Marzke, M. W. (2005). Who made stone tools? In V. Roux & B. Blandine (Eds.), *Stone knapping: The necessary conditions for a uniquely hominin behaviour* (pp. 243–255). McDonald Institute for Archaeological Research.

Marzke, M. W. (2009). Upper-limb evolution and development. *Journal of Bone and Joint Surgery*, 91(4), 26–30.

Marzke, M. W. (2013). Tool making, hand morphology and fossil hominins. *Philosophical Transactions of the Royal Society of London B: Biological Sciences*, 368(1630), 20120414.

Marzke, M. W., Marchant, L. F., McGrew, W. C., & Reece, S. P. (2015). Grips and hand movements of chimpanzees during feeding in Mahale Mountains National P ark, Tanzania. *American Journal of Physical Anthropology*, 156(3), 317–326.

Marzke, M. W., & Wullstein, K. L. (1996). Chimpanzee and human grips: A new classification with a focus on evolutionary morphology. *International Journal of Primatology*, 17(1), 117–139.

Marzke, M. W., Wullstein, K. L., & Viegas, S. F. (1992). Evolution of the power ("squeeze") grip and its morphological correlates in hominids. *American Journal of Physical Anthropology*, 89(3), 283–298.

McGrew, W. C. (2010). Chimpanzee technology. *Science*, 328(5978), 579–580.

Momose, T., Nakatsuchi, Y., & Saitoh, S. (1999). Contact area of the trapeziometacarpal joint. *The Journal of Hand Surgery*, 24, 491–495.

Morley, J., Bucchi, A., Lorenzo, C., & Püschel, T. A. (2022). Characterizing the body morphology of the first metacarpal in the Homininae using 3D geometric morphometrics. *American Journal of Biological Anthropology*, 177(4), 748–759.

Nanno, M., Buford, W. L., Jr., Patterson, R. M., Andersen, C. R., & Viegas, S. F. (2006). Three-dimensional analysis of the ligamentous attachments of the first carpometacarpal joint. *The Journal of Hand Surgery*, 31(7), 1160–1170.

Napier, J. R. (1952). The form and function of the carpo-metacarpal joint of the thumb. *Journal of Anatomy*, 89, 362–370.

Napier, J. R. (1955). The form and function of the carpo-metacarpal joint of the thumb. *Journal of Anatomy*, 89(Pt 3), 362.

Napier, J. R. (1956). The prehensile movements of the human hand. *The Journal of Bone and Joint Surgery (British)*, 38(4), 902–913.

Napier, J. R. (1960). Studies of the hands of living primates. In *Proceedings of the zoological society of London* (pp. 647–657). Blackwell Publishing.

Napier, J. R. (1961). Prehensility and opposability in the hands of primates. *Symposia of the Zoological Society of London*, 5, 115–132.

Napier, J. R. (1993). *Hands*. Princeton University Press.

Neufuss, J., Robbins, M., Baeumer, J., Humle, T., & Kivell, T. (2019). Manual skills for food processing by mountain gorillas in Bwindi impenetrable National Park, Uganda. *Biological Journal of the Linnean Society*, 127(3), 543–562.

Neufuss, J., Robbins, M. M., Baeumer, J., Humle, T., & Kivell, T. L. (2017). Comparison of hand use and forelimb posture during vertical climbing in mountain gorillas (*Gorilla beringei beringei*) and chimpanzees (*Pan troglodytes*). *American Journal of Physical Anthropology*, 164(4), 651–664.

Niewoehner, W. A. (2001). Behavioral inferences from Skhul/Qafzeh earlymodern human hand remains. *Proceedings of the National Academy of Sciences USA*, 98, 2979–2984.

Niewoehner, W. A. (2005). A geometric morphometric analysis of Late Pleistocene human metacarpal 1 base shape. In D. E. Slice (Ed.), *Modern morphometrics in physical anthropology* (pp. 285–298). Springer.

Oksanen, J., Blanchet, F., Friendly, M., Kindt, R., Legendre, P., McGlinn, D. H., Minchin, P. R., O'hara, R. B., Simpson, G. L., Solymos, P., Stevens, M. H. H., Szoecs, E., & Wagner, H. (2018). Vegan: Community Ecology R Package.

Olson, E. C., & Miller, R. L. (1958). *Morphological integration*. University of Chicago Press.

Orr, C. M. (2017). Locomotor hand postures, carpal kinematics during wrist extension, and associated morphology in anthropoid primates. *The Anatomical Record*, 300, 382–401.

Orr, C. M., Leventhal, E. L., Chivers, S. F., Marzke, M. W., Wolfe, S. W., & Crisco, J. J. (2010). Studying primate carpal kinematics in three dimensions using a computed-tomography-based markerless registration method. *The Anatomical Record: Advances in Integrative Anatomy and Evolutionary Biology*, 293(4), 692–709.

Papademetriou, E., Sheu, C. F., & Michel, G. F. (2005). A meta-analysis of primate hand preferences, particularly for reaching. *Journal of Comparative Psychology*, 119(1), 33–48.

Perelle, I. B., & Ehrman, L. (1994). An international study of human handedness: The data. *Behavior Genetics*, 24(3), 217–227.

Pietrobelli, A., Sorrentino, R., Notariale, V., Durante, S., Benazzi, S., Marchi, D., & Belcastro, M. G. (2022). Comparability of skeletal fibulae surfaces generated by different source scanning (dual-energy CT scan vs. high resolution laser scanning) and 3D geometric morphometric validation. *Journal of Anatomy*, 241, 667–682.

Polly, P. D. (2008). Adaptive zones and the pinniped ankle: A three-dimensional quantitative analysis of carnivoran tarsal evolution. In E. J. Sargis & M. Dagosto (Eds.), *Mammalian evolutionary morphology* (pp. 167–196). Springer.

Pouydebat, E., Gorce, P., Coppens, Y., & Bels, V. (2009). Biomechanical study of grasping according to the volume of the object: Human versus non-human primates. *Journal of Biomechanics*, 42(3), 266–272.

Pouydebat, E., Reghem, E., Borel, A., & Gorce, P. (2011). Diversity of grip in adults and young humans and chimpanzees (*Pan troglodytes*). *Behavioural Brain Research*, 218(1), 21–28.

Preuschoft, H., & Chivers, D. J. (Eds.). (2012). *Hands of primates*. Springer Science & Business Media.

R Core Team. (2019). *R: A language and environment for statistical computing*. R Core Development Team.

Rafferty, K. (1990). The functional and phylogenetic significance of the carpometacarpal joint of the thumb in anthropoid primates. (M.A. dissertation). New York University.

Robinson, C., & Terhune, C. E. (2017). Error in geometric morphometric data collection: Combining data from multiple sources. *American Journal of Physical Anthropology*, 164(1), 62–75.

Rohlf, F. J., & Corti, M. (2000). Use of two-block partial least-squares to study covariation in shape. *Systematic Biology*, 49(4), 740–753.

Rohlf, F. J., & Slice, D. (1990). Extensions of the Procrustes method for the optimal superimposition of landmarks. *Systematic Biology*, 39(1), 40–59.

Rolian, C., Lieberman, D. E., & Zermeno, J. P. (2011). Hand biomechanics during simulated stone tool use. *Journal of Human Evolution*, 61(1), 26–41.

Rose, M. D. (1992). Kinematics of the trapezium-1st metacarpal joint in extant anthropoids and Miocene hominoids. *Journal of Human Evolution*, 22(4–5), 255–266.

Sanz, C. M., & Morgan, D. B. (2013). Ecological and social correlates of chimpanzee tool use. *Philosophical Transactions of the Royal Society, B: Biological Sciences*, 368(1630), 20120416.

Scheuer, L., & Black, S. (2000). The upper limb. In C. Cunningham, L. Scheuer, & S. Black (Eds.), *Developmental juvenile osteology* (pp. 272–340). Academic Press.

Schlager, S. (2017). Morpho and Rvcg–shape analysis in R: R-packages for geometric morphometrics, shape analysis and surface manipulations. In G. Zheng, S. Li, & G. Székely (Eds.), *Statistical shape and deformation analysis: Methods, implementation and applications* (pp. 217–256). Academic Press.

Schwarz, R. J., & Taylor, C. (1955). The anatomy and mechanics of the human hand. *Artificial Limbs*, *2*(2), 22–35.

Skinner, M. M., Stephens, N. B., Tsegai, Z. J., Foote, A. C., Nguyen, N. H., Gross, T., Pahr, D. H., Hublin, J. J., & Kivell, T. L. (2015). Human-like hand use in *Australopithecus africanus*. *Science*, *347*(6220), 395–399.

Stephens, N. B., Kivell, T. L., Pahr, D. H., Hublin, J. J., & Skinner, M. M. (2018). Trabecular bone patterning across the human hand. *Journal of Human Evolution*, *123*, 1–23.

Susman, R. L. (1998). Hand function and tool behavior in early hominids. *Journal of Human Evolution*, *35*(1), 23–46.

Tan, A., Tan, S. H., Vyas, D., Malaivijitnond, S., & Gumert, M. D. (2015). There is more than one way to crack an oyster: Identifying variation in Burmese long-tailed macaque (*Macaca fascicularis aurea*) stone-tool use. *PLoS One*, *10*(5), e0124733.

Tocheri, M. W. (2007). *Three-dimensional riddles of the radial wrist: Derived carpal and carpometacarpal joint morphology in the genus Homo and the implications for understanding the evolution of stone-tool related behaviors in hominins.* (Ph.D. Dissertation). Arizona State University.

Tocheri, M. W., Marzke, M. W., Liu, D., Bae, M., Jones, G. P., Williams, R. C., & Razdan, A. (2003). Functional capabilities of modern and fossil hominid hands: Three-dimensional analysis of trapezia. *American Journal of Physical Anthropology*, *122*(2), 101–112.

Tocheri, M. W., Orr, C. M., Jacofsky, M. C., & Marzke, M. W. (2008). The evolutionary history of the hominin hand since the last common ancestor of *Pan* and *Homo*. *Journal of Anatomy*, *212*(4), 544–562.

Tocheri, M. W., Razdan, A., Williams, R. C., & Marzke, M. W. (2005). A 3D quantitative comparison of trapezium and trapezoid relative articular and nonarticular surface areas in modern humans and great apes. *Journal of Human Evolution*, *49*(5), 570–586.

Tocheri, M. W., Solhan, C. R., Orr, C. M., Femiani, J., Frohlich, B., Groves, C. P., Harcourt-Smith, W. E., Richmond, B. G., Shoelson, B., & Jungers, W. L. (2011). Ecological divergence and medial cuneiform morphology in gorillas. *Journal of Human Evolution*, *60*(2), 171–184.

Torigoe, T. (1985). Comparison of object manipulation among 74 species of non-human primates. *Primates*, *26*(2), 182–194.

Trinkaus, E. (1989). Olduvai Hominid 7 trapezial metacarpal 1 articular morphology: Contrasts with recent humans. *American Journal of Physical Anthropology*, *80*, 411–416.

Truppa, V., Carducci, P., & Sabbatini, G. (2019). Object grasping and manipulation in capuchin monkeys (genera *Cebus* and *Sapajus*). *Biological Journal of the Linnean Society*, *127*(3), 563–582.

Tuttle, R. H. (1967). Knuckle-walking and the evolution of hominoid hands. *American Journal of Physical Anthropology*, *26*(2), 171–206.

Tuttle, R. H. (1969). Quantitative and functional studies on the hands of the Anthropoidea. I. The Hominoidea. *Journal of Morphology*, *128*(3), 309–363.

van Leeuwen, T., van Lenthe, G. H., Vereecke, E. E., & Schneider, M. T. (2021). Stress distribution in the bonobo (*Pan paniscus*) trapeziometacarpal joint during grasping. *PeerJ*, *9*, e12068.

van Leeuwen, T., Vanhoof, M. J., Kerkhof, F. D., Stevens, J. M., & Vereecke, E. E. (2018). Insights into the musculature of the bonobo hand. *Journal of Anatomy*, *233*(3), 328–340.

van Leeuwen, T., Vanneste, M., Kerkof, F., D'Agostino, P., Vanhoof, M., Stevens, J., van Lenthe, G. H., & Vereecke, E. E. (2019). Mobility and structural constraints of the bonobo trapeziometacarpal joint. *Biological Journal of the Linnean Society*, *127*(3), 681–693.

Vanhoof, M. J., Galletta, L., De Groote, I., & Vereecke, E. E. (2021). Functional signals and covariation in triquetrum and hamate shape of extant primates using 3D geometric morphometrics. *Journal of Morphology*, *282*(9), 1382–1401.

Wallace, J. M. (2019). Skeletal hard tissue biomechanics. In D. B. Burr & M. R. Allen (Eds.), *Basic and applied bone biology* (pp. 125–140). Academic Press.

Waltenberger, L., Rebay-Salisbury, K., & Mitteroecker, P. (2021). Three-dimensional surface scanning methods in osteology: A topographical and geometric morphometric comparison. *American Journal of Physical Anthropology*, *174*(4), 846–858.

Wiley, D. F., Amenta, N., Alcantara, D. A., Ghosh, D., Kil, Y. J., Delson, E., Harcourt-Smith, W., Rohlf, F. J., St. John, K., & Hamann, B. (2005). Evolutionary morphing. In *Proceedings of IEEE visualization 2005 evolutionary morphing* (pp. 431–438). IEE Computer Society.

Zelditch, M. L., Swiderski, D. L., & Sheets, H. D. (Eds.). (2012). *Geometric morphometrics for biologists: A primer.* Academic press.

SUPPORTING INFORMATION

Additional supporting information can be found online in the Supporting Information section at the end of this article.